IMPURITIES IN UNCONVENTIONAL
SUPERCONDUCTORS

By

LECH S. BORKOWSKI

A DISSERTATION PRESENTED TO THE GRADUATE SCHOOL
OF THE UNIVERSITY OF FLORIDA IN PARTIAL FULFILLMENT
OF THE REQUIREMENTS FOR THE DEGREE OF
DOCTOR OF PHILOSOPHY

UNIVERSITY OF FLORIDA

1995

ACKNOWLEDGEMENTS

TABLE OF CONTENTS

Abstract of Dissertation Presented to the Graduate School
of the University of Florida in Partial Fulfillment of the
Requirements for the Degree of Doctor of Philosophy

IMPURITIES IN UNCONVENTIONAL
SUPERCONDUCTORS

By

LECH S. BORKOWSKI

August 1995

Chairman: Peter J. Hirschfeld
Major Department: Physics

We present a self-consistent theory of superconductors in the presence of
Kondo impurities. The impurity degrees of freedom are treated using the large-
N slave boson technique, leading to tractable equations describing the interplay
between the Kondo effect and superconductivity. We show that for a single
impurity in a superconductor with density of states $N(\omega) \simeq |\omega|^r$, there exists
a critical coupling J_c below which the Kondo effect does not occur. However,
for $r \leq 1$ or $N = 2$ any finite concentration of impurities drives $J_c \to 0$. The
technique is tested on the s-wave case and shown to give good results compared
to other methods for $T_K \gtrsim T_c$. We calculate low temperature thermodynamic
and transport properties for various superconducting states, including isotropic
s-wave and representative anisotropic model states with line and point nodes on
the Fermi surface. The theory provides support for phenomenological models
of resonant impurity scattering in heavy fermion systems.

Motivated by some recent experiments on high-T_c superconductors, we
study properties of superconducting states with "extended s-wave" symmetry.
In the presence of impurities, thermodynamic properties of such states exhibit
gapless behavior, reflecting a residual density of states. While for a range of

impurity concentrations, properties reflecting the density of states alone will be similar to those of d-wave states, transport measurements may be shown to qualitatively distinguish between the two.

We also discuss the effect of two-channel Kondo impurities on superconductivity. In the strong coupling regime such impurities are pairbreakers, in contrast to the ordinary Kondo effect. Measurements of T_c-suppression may help in identifying impurities displaying this more exotic exchange coupling to the conduction band.

CHAPTER 1
INTRODUCTION

The problem of a magnetic impurity in a superconductor has been extensively studied, but is not completely solved because of the difficulty of treating the dynamical correlations of the coupled impurity-conduction electron system together with pair correlations. Generally, the behavior of the system can be characterized by the ratio of the Kondo energy scale in the normal metal to the superconducting transition temperature, T_K/T_c. For $T_K/T_c \ll 1$, conduction electrons scatter from classical spins and physics in this regime can be described by the Abrikosov-Gor'kov theory [1]. In the opposite limit, $T_K/T_c \gg 1$, the impurity spin is screened and conduction electrons undergo only potential scattering. In this regime s-wave superconductors are largely unaffected by the presence of Kondo impurities due to Anderson's theorem [2]. Superconductors with an anisotropic order parameter, e.g. p-wave, d-wave etc., are strongly affected, however, and potential scattering is pair-breaking. The effect of pair breaking is maximal in s-wave superconductors in the intermediate region, $T_K \sim T_c$, while in the anisotropic case it is largest for $T_K/T_c \to \infty$. The interest in the latter class of systems comes from studies of the heavy-fermion and high-T_c superconductors, exhibiting many properties that can be explained by an unconventional order parameter. The word "unconventional" here means that there are broken symmetries in addition to the U(1) symmetry broken in classic superconductor.

1

The Kondo effect is accompanied by the formation of a narrow many-body resonance of width T_K near the Fermi level in the impurity spectral density $N_f(\omega)$. It is reasonable to expect that the opening of a gap Δ in the conduction electron density of states leads through hybridization processes to a similar gap in $N_f(\omega)$, which destroys the Kondo effect if sufficiently large. Withoff and Fradkin [3] pointed out that the two problems of impurity spins coupled to baths of conduction electrons with (a) constant density of states and (b) with a fully developed gap represent two extreme members of a family of problems given by specifying a generalized conduction-electron density of states $N(\omega) = C|\omega|^r, |\omega| < D$, and $0 \leq r < \infty$. Making use of renormalization group arguments as well as explicit calculations for the large degeneracy $\mathrm{SU}(N)$ Kondo (Coqblin-Schrieffer) model, they showed, for $r > 0$, the existence of a critical coupling J_c below which impurities are decoupled from the conduction band and no Kondo effect occurs. The potential physical examples of this phenomenon include unconventional superconducting states with line and point zeroes in the momemtum-dependent gap function, corresponding to densities of states $N(\omega)$ varying as ω and ω^2, respectively. Such states are possibly realized in the heavy fermion superconductors $\mathrm{UPt_3}$, $\mathrm{UBe_{13}}$, $\mathrm{URu_2Si_2}$, $\mathrm{CeCu_2Si_2}$, and $\mathrm{UPd_2Al_3}$. Other examples of systems which have a gapless excitation spectrum under certain conditions are α-Sn, $\mathrm{Pb_{1-x}Sn_xTe}$ at a critical composition, domain walls of PbTe, PbTe-SnTe heterojunctions and graphite.

In the context of heavy-fermion superconductivity, theories of impurity scattering in such states have been given by Ueda and Rice [4] for the case of weak potential scattering, and by Hirschfeld, Vollhardt, and Wölfle [5], and Schmitt-Rink, Miyake, and Varma [6] for strong scattering. Moment formation

was not considered in these theories, but pair breaking still occurs because of the vanishing of the anomalous one-electron impurity-averaged self-energy. The strength of the scattering was parametrized in the latter works by a phase shift δ_0 for s-wave potential scattering of electrons at the Fermi surface. One of the principal results of these treatments was that in the resonant scattering limit, $\delta_0 \rightarrow \pi/2$, corresponding to the single-impurity spin-$\frac{1}{2}$ Kondo effect [7], a "bound-state" resonance was found to form in the superconducting density of states., $N(\omega)$, leading to gapless effects in thermodynamic properties. These are the analogs of the bound states found in discussions of Kondo effects in s-wave superconductors [8].

While this work was begun in anticipation of applications to heavy fermion superconductors, recent measurements of penetration depth [9], photoemission [10, 11], and Josephson tunneling on YBCO and BSSCO [12, 13, 14, 15] have provided evidence that the copper oxide superconductors may be unconventional, possibly d-wave as well. This conclusion remains controversial, however, and experimental tests to distinguish conventional from unconventional pairing are of great current interest. One would like, for example, to develop an understanding of the effect of doping Zn and Ni impurities in the CuO_2 planes. Simple models of Zn and Ni acting as strong and weak potential scatterers in a d-wave superconductor, respectively, are consistent with some experiments at low doping levels [16, 17, 18], but inconsistent with other measurements [19]. Since in some cases Zn impurities appear to possess a magnetic moment at higher temperatures [19], it is of interest to explore whether an s-d type exchange coupling of conduction electrons to an impurity embedded in an unconventional superconductor can describe the range of behavior observed.

In this work we focus initially on basic thermodynamic and transport properties of superconductors doped with Kondo impurities. Our aim is to develop a tractable, self-consistent scheme for the calculation of all basic properties of superconductors using methods known to successfully describe the most difficult aspect of the problem, namely the dynamics of the Kondo impurity. For this reason we have adopted the large-N "slave boson" approach of Barnes [20], Coleman [21], and Read and Newns [22], as this approach is well-known to provide a good description of the spectral properties of the Kondo impurity for sufficiently low temperatures. We emphasize that this description is adequate for most of our purposes $(T_c \lesssim T_K)$ even in the case of spin degeneracy $N = 2$, since the impurity spectral resonance is located at the proper position, i.e. exactly at the Fermi level in this approximation.

Impurity doping experiments in high temperature superconductors motivated us to consider also the effect of nonmagnetic impurities on strongly anisotropic superconductors of the s-wave type. Many experiments probe only the low-lying quasiparticle states of the superconductor, which in the pure system are quite similar for both anisotropic s- and d-wave states with nodes. Nonmagnetic scattering reduces anisotropy of such states without destroying superconductivity, in contrast to the effect the nonmagnetic impurities have on unconventional (non-s-wave) superconducting states. In anisotropic s-wave states having lines of zeroes of the order parameter on the Fermi surface, sometimes called "extended-s" states, scattering on such impurities removes the nodes of the order parameter at certain critical concentration, and induces an energy gap at higher concentrations. This gap should be visible in low-T,

low energy experiments. If the gap is too small to be observed in thermodynamic experiments, one should try transport measurements, e.g. microwave conductivity or thermal conductivty.

In chapter 2 we address questions related to the conditions for the occurence of the Kondo effect in systems with the density of states vanishing at the Fermi level [23]. In chapter 3 we calculate basic properties for both conventional and unconventional superconductors doped with Kondo impurities [24]. Methods of distinguishing strongly anisotropic s-wave superconductors from d-wave superconductors having very similar quasiparticle excitation spectrum are discussed in chapter 4 [25, 26]. In chapter 5 we study the effect of two-channel Kondo impurities on superconductors [27]. Conclusions are presented in chapter 6.

CHAPTER 2
KONDO EFFECT IN SYSTEMS
WITH DENSITY OF STATES
VANISHING AT THE FERMI ENERGY

2.1 <u>Mean-Field Theory of the Single-Impurity Problem</u>

An antiferromagnetic exchange interaction between a magnetic moment of an impurity and a single channel of conduction electrons leads [28, 29] at low temperature to the formation of a spin singlet state. The temperature scale over which the crossover to the low-T state with compensated impurity spin occurs is called the Kondo temperature T_K. The resistivity per impurity as a function of temperature becomes logarithmically divergent when the crossover is reached and saturates at low T, remaining finite at $T = 0$. The low-T state is a Fermi liquid with renormalized Fermi liquid parameters. [28,29] It is well known that any nonzero conduction electron density of states at the Fermi level $N(\epsilon_F)$ leads to the Fermi liquid ground state in the Kondo problem.

What happens in systems with $N(\epsilon)$ vanishing at $\epsilon = \epsilon_F$? Is the ground state of such system containing a dilute ensemble of Kondo impurities metallic or not? If the low energy density of states is described by a power law, $N(\epsilon) \simeq C|\epsilon|^r$, how does the low-temperature, low-energy physics depend on J and r? Examples of systems in which the density of states vanishes with a power law near ϵ_F are unconventional superconductors and semimetals. To have a basic

6

understanding of the problem, Withoff and Fradkin [3] used poor-man's scaling

for the spin-$\frac{1}{2}$ Kondo model

$$
\begin{aligned}
H = \sum_k &\epsilon_k(c_{k\uparrow}^\dagger c_{k\uparrow} + c_{k\downarrow}^\dagger c_{k\downarrow}) + \frac{1}{2}J\sum_{k,k'}(c_{k\uparrow}^\dagger c_{k'\uparrow} - c_{k\downarrow}^\dagger c_{k'\downarrow})S_z \\
&+\frac{1}{2}J\sum_{k,k'}(c_{k\uparrow}^\dagger c_{k'\downarrow}S^- + c_{k\downarrow}^\dagger c_{k'\uparrow}S^+),
\end{aligned}
\tag{2.1}
$$

with the power-law density of states over the whole bandwidth. In poor-man's

scaling [30] one eliminates high-energy states near band edges, reducing the

width of the band to $D - \delta E$. The new effective coupling constant J_{eff} is given

by $J' = J + N(-D)J'\delta E/D + ...$ To restore the original number of states,

$2CD^{1+r}/(1 + r)$, the unit of length is scaled by $(D/D')^{1+r}$. The coupling

constant is changed by $(D'/D)^{1+r}$. To restore the cutoff all quantities with

units of energy are multiplied by D/D'. The renormalized coupling constant

J_R is then

$$
J_r = \left(\frac{D'}{D}\right)^r J' \simeq J + J(JCD^r - r)\delta E/D.
\tag{2.2}
$$

The fixed points are $J = 0$, $J = \infty$, and $J_c = r/(CD^r)$. The last fixed point

is unstable. For $J < J_c$ the effective J flows to 0, and at $J > J_c$ the coupling

constant flows to ∞. In the ordinary Kondo problem with $N(\epsilon) = const.$,

there are only two fixed points: the unstable one at $J = 0$ and the stable one

at $J = \infty$. This is then an indication of qualitatively different physics in the

problem with $r \neq 0$.

Is the result of the poor-man's scaling confirmed by other approaches, e.g.

the large-N approximation? The slave boson approximation is known to give

correct results in the limit of large orbital degeneracy for the ordinary Kondo

problem at low temperature [20,21]. The simplest version of the Anderson Hamiltonian to describe a rare-earth impurity is

$$H = \sum_{km} \epsilon_k c_{km}^\dagger c_{km} + E_f \sum_m f_m^\dagger f_m + U \sum_{m>m'} f_m^\dagger f_m f_{m'}^\dagger f_{m'}$$
$$+ \sum_{km} V_k (c_{km}^\dagger f_m + h.c.). \tag{2.3}$$

The electrons are labelled by their magnetic quantum number $m = -j, ..., j$, with j the total angular momentum, and the impurity degeneracy is $N = 2j+1$. Here we ignore spin-orbit interaction and crystal fields. An electron on one of the degenerate f orbitals at the impurity site has energy E_f. The energy U of the Coulomb repulsion between two impurity f-electrons may be large, e.g. 5-10 eV in the lanthanides. The impurity electrons hybridize with the conduction band with amplitude V_k. Here we assume $V_k = V = const.$, independent of k. When the bare impurity level E_f lies deep below the Fermi energy, such that $|V^2/E_f| \ll D$, and for large on-site Coulomb repulsion, $U \gg V^2/D$, the Hamiltonian (2.3) can be simplified by the Schrieffer-Wolff transformation [31]. The resultant Hamiltonian is the SU(N) generalization of the Kondo model (2.1), also called the Coqblin-Schrieffer model [32],

$$H = \sum_{km} \epsilon_k c_{km}^\dagger c_{km} + \frac{J}{N} \sum_{kk'} \sum_{mm'} c_{km}^\dagger f_{m'}^\dagger f_m c_{km'}. \tag{2.4}$$

The four-fermion term can be eliminated by the Hubbard-Stratonovich transformation. In the limit $N \to \infty$, the saddle-point solution is equivalent to a mean field theory with the boson field playing the role of an (unphysical) order parameter, [22]

$$\sigma = \frac{J}{N} \sum_{km} \langle f_m^\dagger c_{km} \rangle, \tag{2.5}$$

The mean field Hamiltonian now reads

$$H = \sum_{km} \epsilon_k c_{km}^\dagger c_{km} + \sum_{km} \left(\sigma c_{km}^\dagger f_m + h.c. \right) + \epsilon_f (n_f - 1). \qquad (2.6)$$

The auxiliary field and position of the saddle point are obtained by solving two self-consistent equations

$$\left\langle \frac{\partial H}{\partial \epsilon_f} \right\rangle = 0, \qquad (2.7)$$

and

$$\left\langle \frac{\partial H}{\partial \sigma} \right\rangle = 0. \qquad (2.8)$$

For a constant conduction electron density of states, $N(\omega) = N_0 = 1/2D, |\omega| < D$, equations (2.7) and (2.8) were solved by Read and Newns [22], leading to a Lorentzian impurity spectral density centered at ϵ_f, of width $\Gamma = \pi N_0 \sigma^2$. The Kondo temperature in their approach is the width of this low energy resonant level, given by $T_K = \sqrt{\Gamma^2 + \epsilon_f^2} = D \exp(-1/NN_0 J)$. Equation (2.7) can be written as

$$\frac{1}{N} = \int_{-\infty}^{\infty} d\epsilon f(\epsilon) N(\epsilon) N_f(\epsilon), \qquad (2.9)$$

where $N_f(\epsilon) = -\frac{1}{\pi} \text{Im} G_f(\epsilon + i0^+)$ is the impurity density of states, and $G_f^{-1}(\omega) = \omega - \epsilon_f - \Sigma_m(\omega)$ is f-electron Green's function, while equation (2.8) becomes

$$\frac{N\sigma}{J} = \int_{-\infty}^{\infty} d\epsilon f(\epsilon) N(\epsilon) \frac{\epsilon - \epsilon_f}{(\epsilon - \epsilon_f - \text{Re}\Sigma_m(\epsilon))^2 + (\text{Im}\Sigma_m(\epsilon))^2}. \qquad (2.10)$$
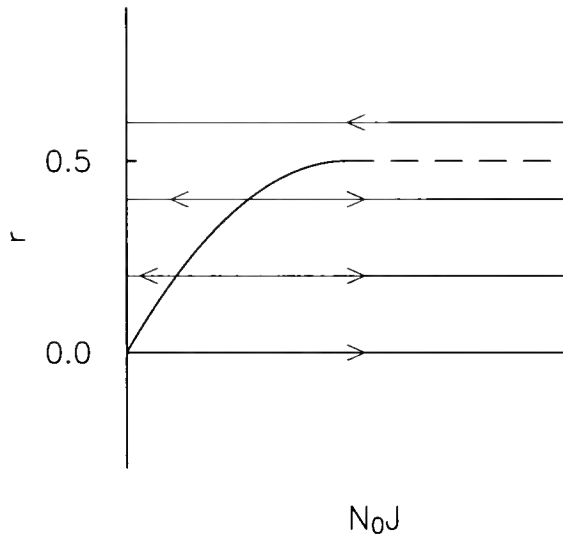
Figure 2.1 Schematic flow diagram for single-channel finite-r Kondo problem obtained from the Numerical Renormalization Group (based on Ref. [26]).

The impurity self-energy Σ_m is

$$\Sigma_m(\epsilon) = \sigma^2 P \int \frac{d\epsilon' N(\epsilon')}{\epsilon' - \epsilon} - i\pi\sigma^2 N(\epsilon). \tag{2.11}$$

The critical coupling obtained from the solution of equations (2.9) and (2.10) corresponds to $\sigma = \epsilon_f = 0$ at $T = 0$. From equation (2.10) the critical coupling is $J_c \simeq r/CD^r$. Both σ and ϵ_f vanish as power-law functions of $|J - J_c|$ near J_c, $\sigma \sim (J - J_c)^{1/r}, \epsilon_f \sim (J - J_c)^{1/r}$. This result comes from the work of Withoff and Fradkin and was later confirmed by us in a numerical solution of equations (2.9) and (2.10). The energy scale for the formation of the singlet is given near the transition by $T_K = (r(J - J_c)/CJJ_c)^{1/r})$.

Recent Numerical Renormalization Group calculations confirm the mean-field result for $r \ll 1$ but differ substantially at larger r [33]. The qualitative form of the flow diagram obtained within NRG is shown in Figure 2.1 . There is a critical exponent, $r_c = 0.5$, such that for $r > r_c$ the Kondo effect does not occur.

In a more realistic treatment, the density of states may be assumed to vary as a power-law over a small energy scale $\Delta \ll D$, $N(\omega) = C|\omega|^r$, and to be constant otherwise, $N(\omega) = C$, for $\Delta < |\omega| < D$. We find that the critical coupling obtained in this case is independent of r, at least for $r \geq 1$, $J_c \simeq 2D/\ln(2D/\Delta)$. It was shown for the problem with a small gap, $N(\omega) = 0$ for $|\omega| < \Delta$, that Quantum Monte Carlo and Numerical Renormalization Group approach yield similar results [34, 35, 36, 37, 38]. The transition associated with the critical ratio T_K/Δ might be observable provided we can tune T_K/Δ. However, it is not a phase transition in the usual sense – it can occur only at $T = 0$. At any finite T the system will not exhibit singularities of the thermodynamic functions but it will have instead a smooth crossover from the impurity spin-singlet-like characteristics to a free moment behavior with increasing Δ. One of the quantities of interest to experimental studies of such a transition is the spin susceptibility. In the ordinary, single channel Kondo problem, the static susceptibility reaches the limit $\chi \to const./T_K$, or $T\chi \to 0$, as $T \to 0$, indicating the screening of the impurity spin by conduction electrons. In a system with a gap in the conduction electron spectrum, the formation of a singlet state is less advantageous energetically and $\chi(T = 0)$ becomes finite as the gap size increases or electron density decreases. Measurements of χ at finite T should indicate a crossover to a Curie-like suceptibility as the singlet ground state becomes unstable.

2.2 NCA Approximation

A more sophisticated version of the large-N approach, the noncrossing approximation (for review of the method see Refs. [39] and [40]) leads to the same conclusions and allows for an extension of the theory into the high
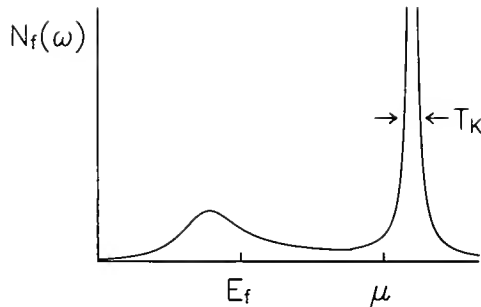
Figure 2.2 Schematic impurity density of states for the Anderson model; μ is the Fermi level and E_f is the position of the bare impurity level. The Kondo temperature is the width of the low energy many-body resonance.

temperature regime, $T \gg T_K$. In NCA one sums all diagrams in the projected perturbation expansion with no crossing conduction electron lines. Here we do the calculations for the Anderson model,

$$
H = \sum_{k,m} \epsilon_k c_{km}^\dagger c_{km} + E_f \sum_m f_m^\dagger f_m + V \sum_{k,m} \left[c_{km}^\dagger f_m b^\dagger + h.c. \right]
$$
$$
+\lambda \left(\sum_m f_m^\dagger f_m + b^\dagger b - 1 \right),
$$

(2.12)

where λ is a Lagrange multiplier enforcing the constraint $n_f + n_b = \sum_m f_m^\dagger f_m + b^+ b = 1$, preventing double occupancy of the impurity site.

The impurity density of states for the Anderson model in the Kondo regime, $-E_f \gg V^2/D$ is shown schematically in Figure 2.2 . The narrow feature at the Fermi level is the Abrikosov-Suhl many-body resonance of width T_K, which controls all low-T thermodynamic and transport properties. The NCA is known to reproduce all qualitative features of the Anderson model spectral function on the scale shown, and fails only below an energy $T_{NCA} \sim T_K^2/D$ [41,40].

The self-energies for the boson and fermion propagators are, respectively (see Figure 2.3),

$$
\Sigma_0(\omega + i0^+) = NV^2 \int_{-\infty}^{\infty} d\epsilon f(\epsilon) N(\epsilon) G_m(\omega + \epsilon + i0^+), \qquad (2.13)
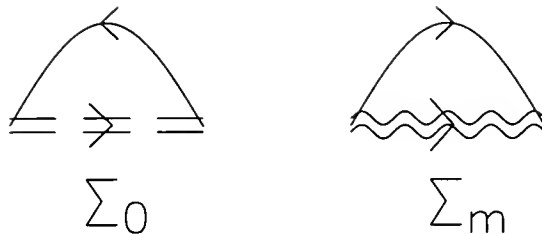$$

Figure 2.3 Self-energies for the empty impurity f-level (slave boson), Σ_0, and for the occupied f-level (fermion), Σ_m.

and

$$\Sigma_m(\omega + i0^+) = V^2 \int_{-\infty}^{\infty} d\epsilon (1 - f(\epsilon)) N(\epsilon) G_0(\omega - \epsilon + i0^+). \qquad (2.14)$$

At $T = 0$ and for integer r equations (2.13) and (2.14) can be tranformed into a system of differential equations and can be solved by a generalization of the method used by Inagaki [42] and later by Kuramoto and Kojima [43]. The solution of NCA equations at finite temperature for $r = 0$ is discussed in detail e.g. in a review by Bickers [40].

Here we only show the results for the spin susceptibility. The temperature dependence of the static spin susceptibility exhibits a crossover from the high-T free-moment behavior to the low-T strong coupling regime.

The levelling off of the $r = 0$ curve in Figure 2.4 indicates a crossover to the low temperature Fermi liquid state, as confirmed by the Bethe Ansatz [44] and NRG solutions of the problem [29]. Figure 2.4 captures the essence of the problem correctly: increasing r leads to lower T_K.
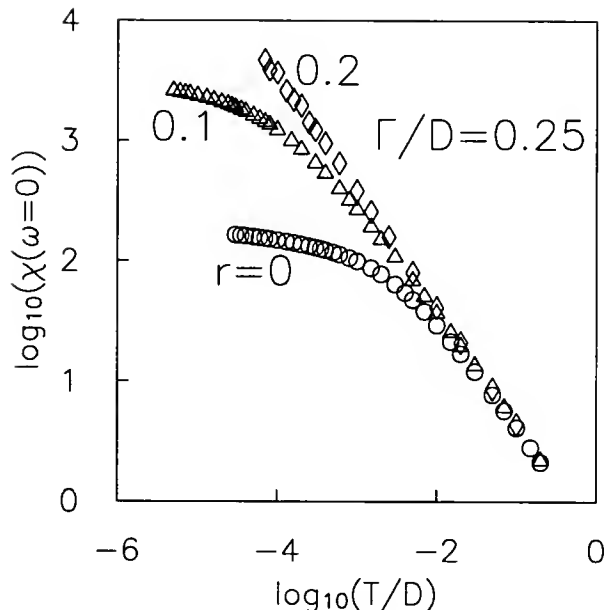
Figure 2.4 The spin susceptibility for $r = 0$ (circles), 0.1 (triangles), 0.2 (rhombuses); $N = 2$, $\Gamma/D = 0.25$, $E_f/D = -0.67$. The Kondo temperature is $T_K/D = (\Gamma/\pi D)^{1/N} \exp(\pi E_f/N\Gamma)$, and for $r = 0$, $\Gamma/D = 0.25$, it is approximately equal to $T_K/D \simeq 4.2 \times 10^{-3}$.

In Figures 2.5 , 2.6 , 2.7 , and 2.8 we show $\log \chi(T, \omega = 0)$ for $r = 0.05, 0.1$, 0.15, 0.2, and several values of hybridization. We clearly see a decrease of T_K with decreasing Γ in each set of data.

Figure 2.9 shows $\log(T\chi)$ for two lowest values of Γ from each of the Figures 2.5-2.8. In the case of $r = 0.2$ the transition from the screened to the finite moment regime is rather convincingly demonstrated. For $r = 0.05, 0.1$, and 0.15, the values of Γ seem not to be far from the critical ones, although the transition is not reached. How does Γ_c obtained in NCA compare to the critical coupling obtained in the poor man's scaling and in the mean field approach? Remembering that in the CS limit $J = V^2/E_f = \Gamma/\pi E_f$, we find that $N_0 J_{c,\mathrm{NCA}}(r = 0.2) \simeq 0.16$, where we assumed $\Gamma_c \simeq 0.32$ for $r = 0.2$.

Figure 2.5 The spin suceptibility for $r = 0$ and $r = 0.05$; $N = 2, E_f/D = -0.67$. For $r = 0$ and $\Gamma = 0.14, 0.15, 0.175,$ and 0.2, the Kondo temperature is $T_K/D \simeq 1.15 \times 10^{-4}, 1.96 \times 10^{-4}, 5.77 \times 10^{-4},$ and 1.31×10^{-3}, respectively.

The critical coupling $N_0 J_c$ for $r = 0.2$, in both the mean field and the NRG approach is approximately 0.2.

Figure 2.6 The spin suceptibility for $r = 0$ and $r = 0.1$; $N = 2$, $E_f/D = -0.67$. For $r = 0$ and $\Gamma/D = 0.2, 0.225, 0.25$, and 0.275, the Kondo temperature is $T_K/D \simeq 1.31 \times 10^{-3}, 2.5 \times 10^{-3}, 4.2 \times 10^{-3}$, and 6.44×10^{-3}, respectively.

Figure 2.7 The spin suceptibility for $r = 0$ and $r = 0.15$; $N = 2$, $E_f/D = -0.67$. For $r = 0$ and $\Gamma/D = 0.3, 0.35, 0.4, 0.5$, and 0.6, the Kondo temperature is $T_K/D = 9.3 \times 10^{-3}, 1.65 \times 10^{-2}, 2.6 \times 10^{-2}, 4.9 \times 10^{-2}$, and 7.6×10^{-2}, respectively.
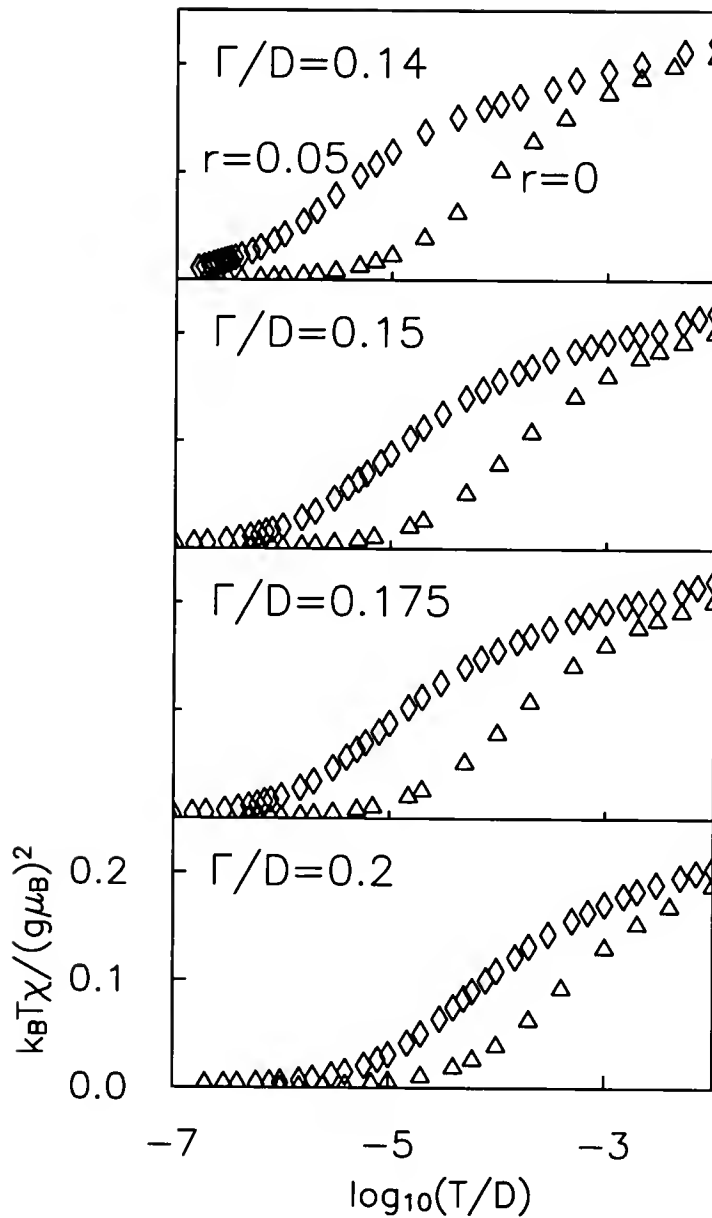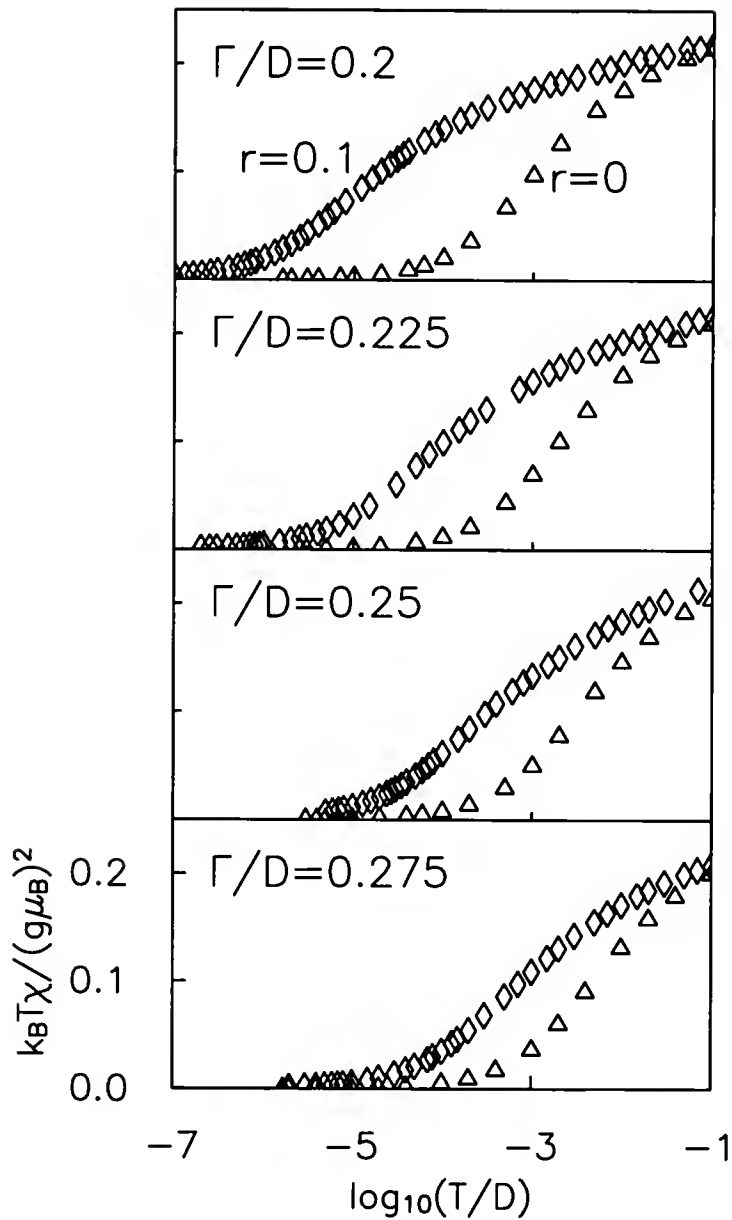
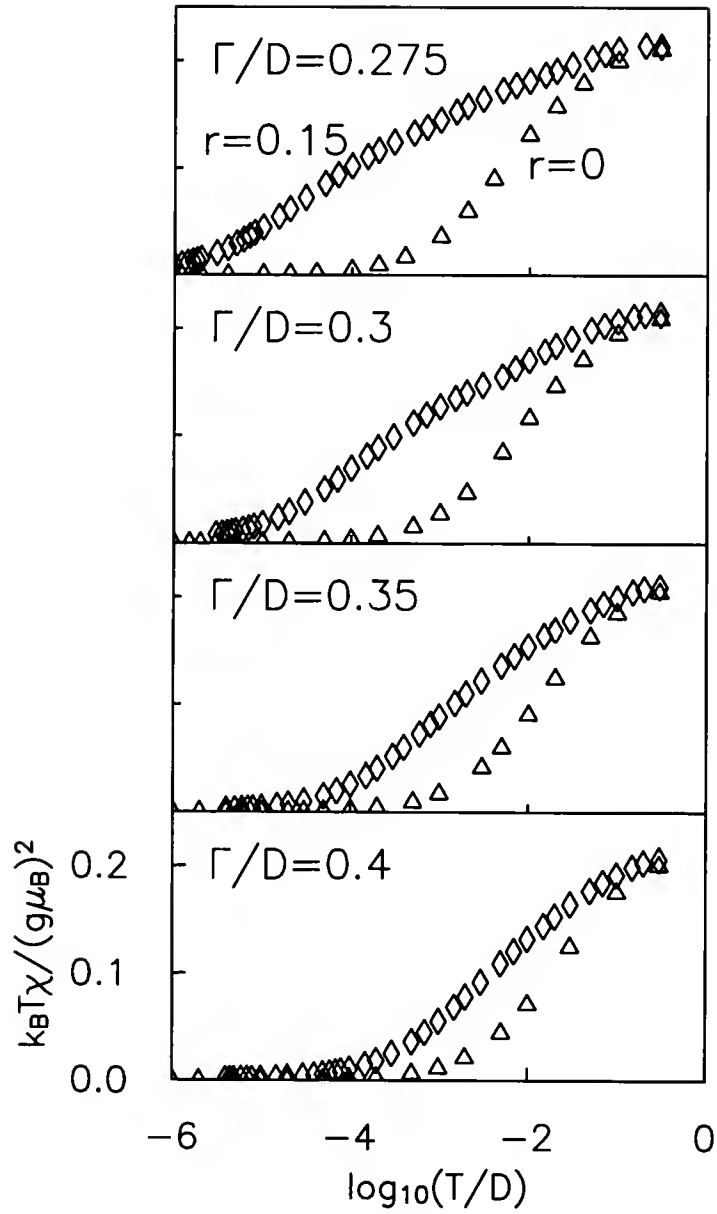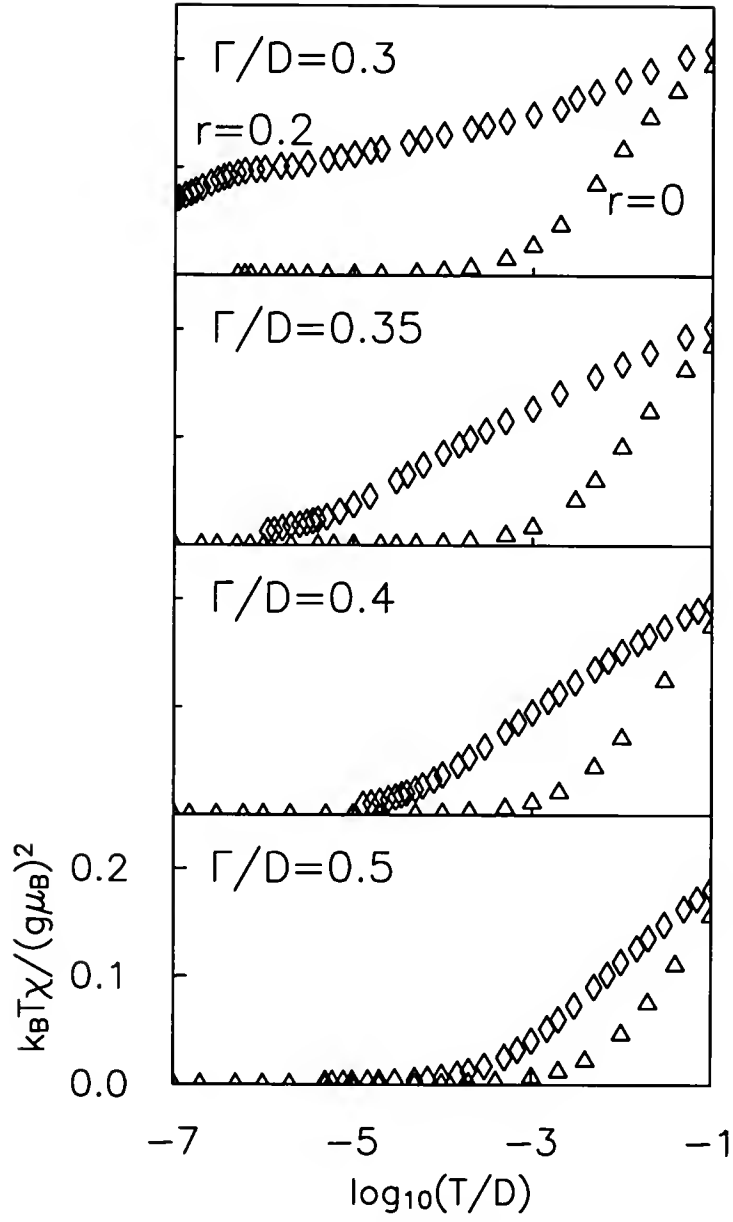**Figure 2.8** The spin suceptibility for $r = 0$ and $r = 0.2$; $N = 2$, $E_f/D = -0.67$. For $r = 0$ and $\Gamma/D = 0.3, 0.35, 0.4$, and 0.5, the Kondo temperature is $T_K/D = 9.3 \times 10^{-3}, 1.65 \times 10^{-2}, 2.6 \times 10^{-2}$, and 4.9×10^{-2}, respectively.
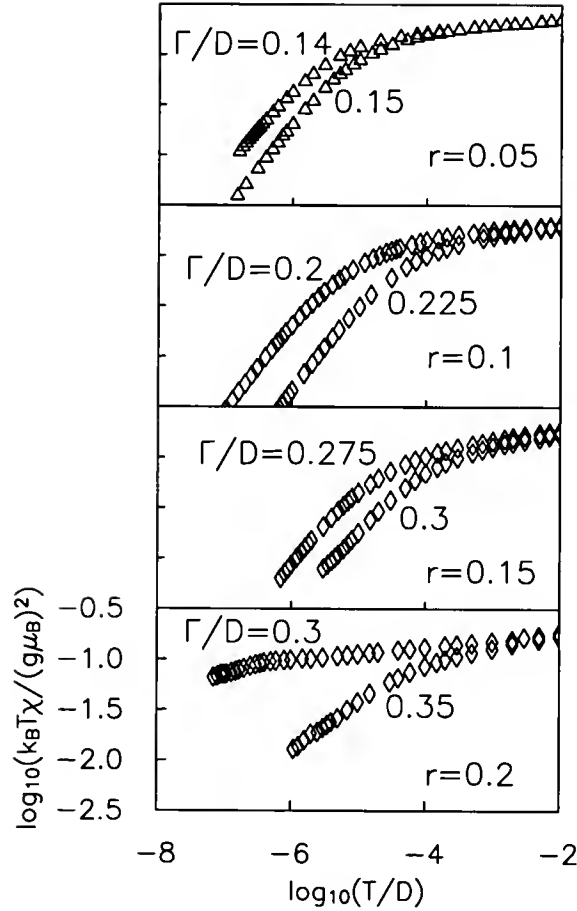
Figure 2.9 Logarithm of $T\chi$ for two lowest values of Γ from each set of data shown in Figures 2.5-2.8.

2.3 Kondo Impurity in a Superconductor

One of the obvious applications of the theory discussed in the previous section is the problem of a Kondo impurity in a superconductor. A superconductor differs from a normal metal not only through the gap in the density of states, but also through the existence of off-diagonal long range order described by the order parameter $\Delta(k)$. To analyze the problem we start from the SU(N) Coqblin-Schrieffer Hamiltonian, already introduced in equation (2.4), and add a simple BCS-like pairing of electrons on opposite sides of the Fermi sphere,

$$H = \sum_{k,m} \epsilon_k c^\dagger_{km} c_{km} + \frac{J}{N} \sum_{k,k'} \sum_{m,m'} c^\dagger_{km} f^\dagger_{m'} f_m c_{km'} + \sum_{k,m} \left[\Delta(k) c^\dagger_{km} c^\dagger_{-k-m} + h.c. \right],$$

(2.15)

We now generalize the procedure of Read and Newns [22] to include super-conducting correlations in the functional integral representation of (2.15). The saddle-point approximation to this theory is equivalent in the $N \to \infty$ limit to a mean-field theory of (2.15) with mean-field amplitude $\sigma = (J/N) \sum_{km} \langle c_m f^\dagger_m \rangle$ and Lagrange multiplier ϵ_f implementing the average constraint. It leads to the two equations

$$\frac{1}{N} = -\mathrm{Im} \int_{-\infty}^{\infty} d\omega f(\omega) \frac{1}{2} \mathrm{Tr}\left[(\tau_0 + \tau_3) \mathbf{G}_f(\omega + i0^+) \right],$$

(2.16)

and

$$\frac{1}{J} = \mathrm{Im} \int_{-\infty}^{\infty} d\omega f(\omega) \frac{1}{2} \mathrm{Tr}\left[(\tau_0 + \tau_3) \mathbf{G}^0(k, \omega + i0^+) \mathbf{G}_f(\omega + i0^+) \right],$$

(2.17)

where $\mathbf{G}^0$ denotes the conduction electron Green's function in the pure super-conductor and $\mathbf{G}_f$ is the full impurity Green's function, given by

$$\mathbf{G}_f^{-1}(\omega) = \omega \tau_0 - \epsilon_f \tau_3 - \mathbf{\Sigma}_f(\omega).$$

(2.18)

Both are matrices in particle-hole space spanned by the Pauli matrices τ_i,

$$\mathbf{G} = \begin{pmatrix} G & F \\ F^\dagger & G^* \end{pmatrix} \quad \text{and} \quad \mathbf{G}_f = \begin{pmatrix} G_f & F_f \\ F_f^\dagger & G_f^* \end{pmatrix}$$

(2.19)

and $\mathbf{\Sigma}_f(\omega) = \sigma^2 \sum_k \mathbf{G}(k, \omega)$ is the impurity self-energy. In the supercon-ducting state, we must solve the full saddle-point equations (2.13) and (2.14) together with Dyson's equations for $\mathbf{G}_f$ and $\mathbf{G}$ as well as the gap equation

$$\Delta(k) = \int_{-\infty}^{\infty} d\omega f(\omega) \sum_{k'} V_{kk'} \text{Tr} \frac{1}{2} \left[(\tau_1 - i\tau_2) \mathbf{G}(k', \omega) \right]. \qquad (2.20)$$

Let us focus first on the case of a single impurity. We also consider the case of small N, despite the fact that Eqs (2) and (3) are strictly valid only in the large-N limit. Here we adopt the point of view that, since the saddle point for $N = 2$ is known to reproduce the correct analytic low-temperature normal-state behavior [7] of the f resonance, including its position at $\epsilon_f = 0$, the $N = 2$ theory will provide a good starting point for a description of $T_K \gg T$ regime. For the superconducting order parameter we take for simplicity the usual isotropic s-wave state $\Delta(k) = \Delta$, model p-wave states with lines ["polar", $\Delta(k) = \Delta_0 \hat{k}_z$] and points of nodes ["axial", $\Delta(k) = \Delta_0(\hat{k}_x + i\hat{k}_y)$] on the Fermi surface, with densities of states varying at low energies $\omega \ll \Delta_0$ as 0, ω and ω^2, respectively. The critical coupling J_c in this case [3] is now defined to be that J for which $\sigma = \epsilon_f = 0$ is the only solution of Eqs. (2) and (3), with $\mathbf{G}(k, \omega)$ replaced by $\mathbf{G}^0(k, \omega)$. We note that to show that σ and ϵ_f always scale to zero together at the transition for $N < \infty$ requires a careful analysis of impurity bound states in $A_f(\omega)$, which occur in the gap and outside the band edges. It follows from this analysis and from Eq. (3) that J_c is independent of N. For the (unphysical) case $\Delta_0 = D$ we recover the WF $r = 1$ result, $J_c/D = 1$, for the polar state, while for the axial state we find $J_c/D = 1.44$. This differs slightly from the WF $r = 2$ result $J_c/D = 1.33$, as the axial density of states deviates from pure ω^2 behavior at larger energies. In the physical limit $\Delta_0 \ll D$, we obtain $J_c \simeq 2D/\ln(2D/\Delta_0)$ for axial, polar and isotropic s-wave states. In Figure 2.10 we plot J_c vs Δ_0/D for all three states.
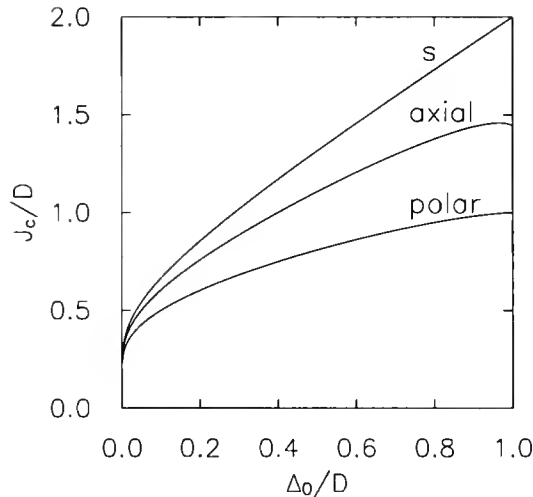
Figure 2.10 Critical coupling J_c/D for one impurity as a function of the order parameter amplitude.

To study the case of finite impurity concentrations, we calculate self-consistent Green's functions averaged over impurity positions in the usual way, leading to $\mathbf{G}_f^{-1}(\omega) = \bar{\omega}\tau_0 - \epsilon_f\tau_3$, and $\mathbf{G}^{-1}(\omega) = \tilde{\omega}\tau_0 - \epsilon_k\tau_3 - \Delta(k)\tau_1$, where

$$\bar{\omega} = \omega + \Gamma \left\langle \tilde{\omega}/\left(\Delta^2(k) - \tilde{\omega}^2\right)^{1/2}\right\rangle_{\hat{k}} \tag{2.21}$$

and

$$\tilde{\omega} = \omega + a\Gamma\bar{\omega}/(-\bar{\omega}^2 + \epsilon_f^2). \tag{2.22}$$

Here $a = \bar{n}T_{c0}N/2\pi$, and $\bar{n} = n/T_{c0}N_0$ is the scaled impurity concentration. In general, $\mathbf{G}_f^{-1}$ and $\mathbf{G}^{-1}$ will also contain additional off-diagonal renormalizations, which vanish in the p-wave case considered here.

An interesting consequence of the self-consistent treatment of impurity scattering is that the conclusions of WF regarding the existence of a critical exchange coupling J_c based on a single-impurity analysis are modified. It is clear from physical considerations or from Eqs. (2) and (3) that the Kondo effect occurs for all $J > 0$ whenever the density of states at the Fermi level

$N(0)$ is finite. Since in the polar state any finite impurity concentration $\bar{n}$ may be shown to lead self-consistently to $N(0) > 0$, as also found in Refs. [4,5,6], the transition discussed by WF does not take place. This may easily be seen by solving the equations for $\tilde{\omega}$ and $\bar{\omega}$ at $\omega = 0$, with $\mathrm{Im}\tilde{\omega}(0) > 0$. A closer analysis shows that $J_c = 0$ for all superconducting states with density of states $N(\omega) \sim |\omega|^r$ for $\omega \ll \Delta_0$, $r \leq 1$. In the axial state ($r = 2$), and indeed for any state with $1 < r < \infty$, the cases $N = 2$ and $N > 2$ are qualitatively different. If $N > 2$, a critical concentration is required to create a gapless state $N(0) > 0$, and thus drive $J_c \to 0$. However, when the bound state is located exactly at the Fermi surface ($N = 2, \epsilon_f = 0$), we find again a finite density of states $N(0)$ for any finite concentration. These results are also in accord with earlier studies [5,6], where the phenomenological phase shift δ_0 is crudely given here by $\cot^{-1}\epsilon_f/\Gamma$.

Our results suggest that the transition discussed by WF might be observable in ordinary superconductors doped with Kondo impurities with spin degeneracy $N > 2$, e.g., Ce. For $N = 2$ we have shown that effective Kondo temperature in the superconducting state is reduced but never vanishes. Nevertheless, in relatively clean systems deviations in thermodynamic properties per impurity from those of the pure superconductor may be qualitatively similar to what one might expect from a WF-type analysis if the effective T_K is driven to zero. The theory presented here provides an easily tractable framework to calculate such properties, as well as transport coefficients, in the superconducting state. Furthermore, it improves upon phenomenological theories [5,6] by including a Kondo impurity description of the energy dependence of scattering phase shifts.

CHAPTER 3
PHYSICAL PROPERTIES OF MAGNETIC
IMPURITIES IN SUPERCONDUCTORS

3.1 Introduction

In this chapter we focus on basic thermodynamic and transport properties of superconductors doped with Kondo impurities. We would like to examine these properties both near T_c and at $T \ll T_c$, when the superconducting gap is fully developed. The presence of bound states within the superconducting gap strongly modifies the low-T behavior. This is true for both conventional and unconventional superconductors. After testing our approach and providing some new results for the s-wave case we discuss results for unconventional superconductors. We emphasize that the large-N description is adequate for most of our purposes ($T_c \lesssim T_K$) even in the case of spin degeneracy $N = 2$, since the impurity spectral resonance is located at the proper position, i.e. exactly at the Fermi level in this approximation.

As in chapter 2, we use the large-N slave boson technique for the $SU(N)$ Anderson model describing an N-fold degenerate band of conduction electrons, c_{km}, $m = 1, ... N$ with energy ϵ_k hybridizing through matrix element V with a localized impurity state f_m. In general this Hamiltonian contains a term with the Coulomb repulsion U between two electrons present at the impurity simultaneously. In many compounds U is large and for the purpose of studying the low temperature physics we will assume $U = \infty$. The on-site repulsion term

24

is then absent, but a constraint is added to ensure that the system remains in the physical part of the Hilbert space. The conduction band is assumed to have a constant density of states in its normal state, $N(\omega) = 1/2D = N_0$. We also include a BCS-like pairing term of electrons on opposite sides of the Fermi sphere,

$$
\begin{aligned}
H = & \sum_{k,m} \epsilon_k c^\dagger_{km} c_{km} + E_f \sum_m f^\dagger_m f_m + V \sum_{k,m} [c^\dagger_{km} f_m b + h.c.] \\
& + \sum_{k,m} [\Delta(k) c^\dagger_{km} c^\dagger_{-k-m} + h.c.] + \lambda(\sum_m f^\dagger_m f_m + b^\dagger b),
\end{aligned}
\tag{3.1}
$$

In the limit $E_f \to -\infty$, $N_0 V^2/E_f$ =const, Equation (3.1) reduces to the Coqblin-Schrieffer Hamiltonian with pairing studied in section 2.3. Here we have chosen the more general form (3.1) to study deviations from single occupancy, $n_f \neq 1$, although we do not attempt to explore the fully developed mixed valent regime.

The mean field approximation to this model, with mean-field amplitude $\langle b \rangle$, leads to the two equations

$$
\frac{1}{N} = -\text{Im} \int_{-\infty}^{\infty} d\omega f(\omega) \frac{1}{2} \text{Tr}(\tau_0 + \tau_3) \mathbf{G}_f(\omega + i0^+),
\tag{3.2}
$$

and

$$
\frac{E_f - \epsilon_f}{V^2} = \text{Im} \int_{-\infty}^{\infty} d\omega f(\omega) \frac{1}{2} \text{Tr}\left[(\tau_0 + \tau_3)(\mathbf{G}^0(k, \omega + i0^+) \mathbf{G}_f(\omega + i0^+)) \right],
\tag{3.3}
$$

which determine $\langle b \rangle$ and ϵ_f, the latter being the position of the resonant state. Equations (3.2) and (3.3) should be solved self-consistently together with the gap equation (2.20). The full conduction electron Green's function $\mathbf{G}$ and

Figure 3.1 Dyson equations for the conduction electron and impurity Green's functions. Double lines are full Green's functions; single lines are bare Green's functions ($V = 0$).

the impurity Green's function $\mathbf{G}_f$ are calculated from the diagrams shown in Figure 3.1 , yielding

$$\mathbf{G}(\omega)^{-1} = \mathbf{G}^0(\omega)^{-1} - \mathbf{\Sigma}(\omega) = \tilde{\omega}\tau_0 - \epsilon_k\tau_3 - \tilde{\Delta}(k)\tau_1, \qquad (3.4)$$

$$\mathbf{G}_f(\omega)^{-1} = \mathbf{G}^0_f(\omega)^{-1} - \mathbf{\Sigma}_f(\omega) = \bar{\omega}\tau_0 - \epsilon_f\tau_3 - \bar{\Delta}\tau_1. \qquad (3.5)$$

The Green's functions are now averaged over impurity positions in the usual way. The renormalized frequencies are calculated self-consistently from the Dyson equations,

$$\tilde{\omega} = \omega + \alpha\bar{\omega}/(-\bar{\omega}^2 + \epsilon^2{}_f + \bar{\Delta}^2), \qquad (3.6)$$

and

$$\bar{\omega} = \omega + \Gamma \left\langle \tilde{\omega} / \left(\tilde{\Delta}^2(k) - \tilde{\omega}^2 \right)^{1/2} \right\rangle_{\hat{k}}. \tag{3.7}$$

Here $\alpha = N\bar{n}\Gamma T_{c0}/2\pi$, $\bar{n} = n/N_0 T_{c0}$ is the scaled impurity concentration, and $\langle ... \rangle_{\hat{k}}$ is a Fermi surface average. The off-diagonal renormalizations are

$$\tilde{\Delta}(k) = \Delta(k) + \alpha \bar{\Delta} / (-\bar{\omega}^2 + \epsilon^2{}_f + \bar{\Delta}^2), \tag{3.8}$$

and

$$\bar{\Delta} = \Gamma \left\langle \tilde{\Delta}(k) / \left(\tilde{\Delta}^2(k) - \tilde{\omega}^2 \right)^{1/2} \right\rangle_{\hat{k}}. \tag{3.9}$$

In superconductors with order parameters where the Fermi surface average in equation (3.9) vanishes, off-diagonal corrections vanish and $\tilde{\Delta}(k) = \Delta(k)$. This class includes but is not limited to odd-parity superconducting states. The energy scale Γ is the renormalized resonance width, $\Gamma = \langle b \rangle \pi N_0 V^2$. The low-temperature Kondo scale in the large-N slave boson theory is given by $T_K \equiv \sqrt{\Gamma^2 + \epsilon_f{}^2}$. Although the width of the actual spectral feature corresponding to the Abrikosov-Suhl resonance is modified below T_c, in what follows we will normalize all quantities with respect to this T_K, evaluated from equations (3.2) and (3.3) with $\Delta = 0$ at $T = 0$. In the regime of principal interest, $T_K > T_c$, corrections to this definition are small in any case.

The early history of the problem of a Kondo impurity in an s-wave superconductor has been reviewed by Müller-Hartmann [45]. Abrikosov and Gor'kov first discussed the pair-breaking effects of magnetic impurities weakly coupled via exchange interactions to conduction electrons [1]. Shiba [46] extended this approach to treat strong scattering by classical spins, using the t-matrix approximation, and showed the existence of bound states in the gap.

At finite concentration of impurities the bound states were found to form an impurity band whose width and center scaled with impurity concentration and exchange strength. These early works neglected the dynamical screening of the localized spin by the conduction electron gas. These effects were incorporated by Müller-Hartmann and Zittartz [47], adopting an equation of motion decoupling scheme previously used by Nagaoka [48] to calculate the dynamical spin correlations in the normal state. This approach correctly reproduced results in the Abrikosov-Gor'kov limit, $T_K/T_c \to 0$, and made the remarkable prediction of a reentrant superconducting phase if $T_K \ll T_c$, subsequently observed in experiments on $La_{1-x}Ce_xAl_2$ [49, 50, 51]. The failure of the decoupling scheme used to capture the correct crossover to Fermi liquid behavior in the normal state as $T \to 0$ invalidated the Müller-Hartmann–Zittartz approach in the low temperature regime $T_K > T_c$, however.

The physics of the Fermi liquid regime, $T_K/T_c \to \infty$, was studied by Matsuura, Ichinose and Nagaoka [52] and by Sakurai [53] by extending the Yamada-Yosida theory [54] to the superconducting state. They obtained an exponential T_c-suppresssion with increasing impurity concentration $\bar{n}$, $T_c \simeq T_{c0}\exp(-p\bar{n}/\lambda)$, where λ is the BCS dimensionless coupling constant, and p is a constant of order unity. This is commonly referred to as "pair-weakening" as opposed to pair-breaking, since the effective superconducting coupling constant is reduced due to correlations on the impurity site. The exponential form breaks down for concentrations sufficiently close to a critical $\bar{n}_c$, for which $T_c = 0$. In this regime the reentrant behavior found by Müller-Hartmann and Zittartz does not occur. A further characteristic signature of the Fermi liquid regime is the reduced specific heat jump, $C^* \equiv (\Delta C/\Delta C_0)/(T_c/T_{c0}))|_{T_c=T_{c0}}$

which is always less than one [53, 55], in contrast to the high temperature regime.

Not surprisingly, qualitatively similar results were obtained by other early workers for Kondo and Anderson impurities using a variety of other approaches [45]. More recent treatments include the use of a self-consistent large-N [56], Monte Carlo [57] and NRG methods [58]. Schlottman [59] has treated the mixed–valence regime using Brillouin-Wigner perturbation theory. Out of these efforts has evolved a qualitatively consistent picture of the effect of Kondo impurities on the superconducting transition [60], but little understanding of the low-temperature properties of Kondo-doped superconductors because of the difficulty of the calculations involved. In the next section we show that the current theory reproduces the known effects of Kondo impurities on the critical temperature, specific heat jump and bound states spectrum of an s-wave superconductor.

3.2 <u>Results for Conventional Superconductors</u>

3.2.1 <u>Suppression of the Critical Temperature</u>

The simplest and most direct effect of impurity scattering on a superconductor is the suppression of the critical temperature. Scattering from impurities with internal quantum-mechanical degrees of freedom leads to deviations from the classic Abrikosov-Gor'kov prediction for the dependence of T_c on impurity concentration [1]. These effects depend sensitively on the low-energy behavior of the self-energy $\Sigma(\omega)$, which enters the linearized gap equation, obtained from equation (2.20) near T_c,
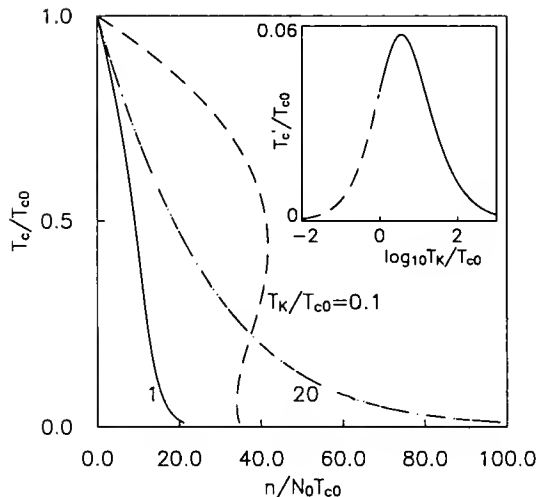
Figure 3.2 The critical temperature for an s-wave superconductor as a function of impurity concentration. The inset shows the slope of this dependence evaluated at $T_c = T_{c0}$.

$$\ln(T_c/T_{c0}) = 2\pi T_c \sum_{n \geq 0} \frac{1}{\omega_n(1 + \alpha/B(\omega_n))} - \sum_{n \geq 0} \frac{1}{n + 1/2}, \tag{3.10}$$

where $B(\omega_n) = (\omega_n + \Gamma)^2 + \epsilon_f{}^2$.

The slope of the T_c-suppression evaluated at $\bar{n} = 0$ is therefore

$$\left(\frac{1}{T_{c0}} \frac{dT_c}{d\bar{n}} \right)_{\bar{n}=0} = -\frac{N}{2\pi} \sum_{n \geq 0} \frac{\Gamma T_{c0}}{(n + 1/2)B(\omega_n)}. \tag{3.11}$$

In an insert to Figure 3.2 , we have plotted a numerical evaluation of equation (3.11) for an s-wave superconductor. Note the curve is drawn with a broken line for small T_K/T_{c0} to reflect the fact that the slave boson mean field theory is expected to break down there. The maximum of the T_c-suppression is found to occur at $T_K \simeq 3T_c$, similar to the NCA result [56]. The early high-temperature theory of Müller-Hartmann and Zittartz [47] locates this maximum at $T_K/T_c \simeq 12$, whereas in the more recent Monte Carlo calculation

[57] for the symmetric Anderson model with finite U the maximum slope of the T_c-suppression is at $T_K \simeq T_c$. Unfortunately a direct quantitative comparison with the latter work is not possible, as the simulation is not performed in the fully developed Kondo regime.

The present theory predicts an exponential decrease of T_c at small concentrations, in agreement with other theories of the Fermi liquid regime [53,55],

$$T_c \simeq T_{c0}\exp\left[-\frac{\alpha}{T_K{}^2}\Psi(T_K/2\pi T_{c0})\right] \simeq T_c\left(1 - \frac{\alpha}{T_K{}^2}\ln(T_K/T_{c0})\right), \qquad (3.12)$$

where Ψ is the digamma function. In Refs. [61] and [53] the initial suppression of T_c is proportional to $\ln^2(T_K/T_{c0})$. A full evaluation of equation (3.11) for arbitrary concentrations and various values of the ratio T_K/T_c is shown in Figure 3.2 . It is interesting to note that the theory reproduces the reentrant behavior characteristic of the high temperature regime [45] although we do not expect the theory to be accurate in this case (dashed line).

As is evident in the Figure the current theory predicts no critical concentration n_c for which $T_c = 0$. This is a subtle point discussed by Sakurai [53], who suggests that a failure to include the dynamics of magnetic scattering by states close to the Fermi surface can lead to such an effect. Such processes are included in the finite-U perturbation theory through Coulomb vertex corrections to the impurity averaged pair correlation function. In our $U = \infty$ theory, such vertex corrections arise first in leading order $1/N$ corrections due to the exchange of slave bosons, whose dynamics are neglected in this work. We expect that effects arising from the absence of these fluctuations in the theory will be quantitatively small for $T_c \lesssim T_K$, except for impurity concentrations so large such that $T_c \ll T_{c0}$.

3.2.2 Position of Bound States

For conventional superconductors, $\Delta(k) = \Delta$, equations (3.7) and (3.9) are simply

$$\bar{\omega} = \omega + \Gamma \frac{\tilde{\omega}}{\left(\tilde{\Delta}^2 - \tilde{\omega}^2\right)^{1/2}}, \tag{3.13}$$

and

$$\bar{\Delta} = \Gamma \frac{\tilde{\Delta}}{\left(\tilde{\Delta}^2 - \tilde{\omega}^2\right)^{1/2}}. \tag{3.14}$$

It is obvious from equation (3.14) that a finite gap in the conduction electron spectrum induces a gap in the impurity spectrum, $N_f(\omega) = -\frac{1}{\pi}\mathrm{Im}G_f(\omega+i0^+)$. When the Abrikosov-Suhl resonance, which develops at temperatures below T_K, falls in the superconducting gap, bound states appear in the conduction electron spectrum. These peaks are placed symmetrically relative to the center of the gap and their spectral weight depends on T_K/T_c and on impurity concentration.

The density of states for $N = 2$ and $N = 4$, exhibiting pronounced peaks at the bound state positions, is shown in Figure 3.3 . Figure 3.4 shows $N(\omega)$ in the Coqblin-Schrieffer limit for $N = 2$ and several values of Γ. In the high-temperature regime the bound states emerge from the edges of the gap and move towards the center of the gap as T_K/T_c increases [62]. In the low-temperature limit, the bound states disappear into the gap edges again [61]. Recently, Shiba et al. [58] studied the position of bound states in the gap in an s-wave superconductor using the numerical renormalization group (NRG). Their results cover both the high- and low-temperature limits reliably. The
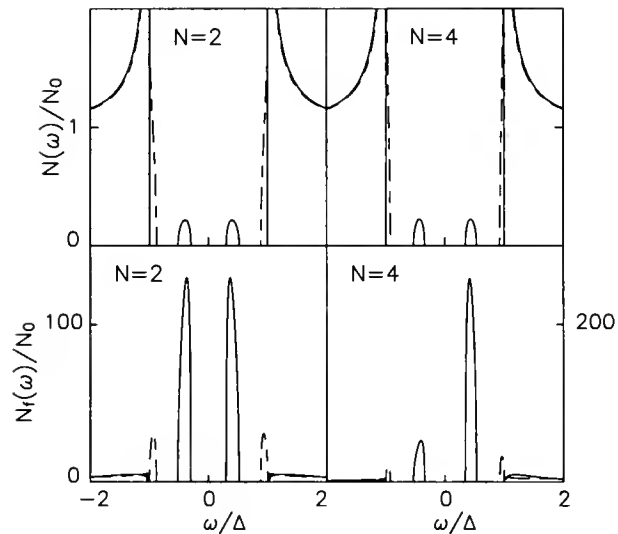
Figure 3.3 Conduction electron and impurity spectral functions in the Coqblin-Schrieffer limit in an s-wave superconductor for $N = 2$ and $N = 4$. The solid and dashed lines correspond to $T_K = T_c$, and $T_K = 10T_c$, respectively. The concentration of impurities in all cases is $\bar{n} = 0.4$.

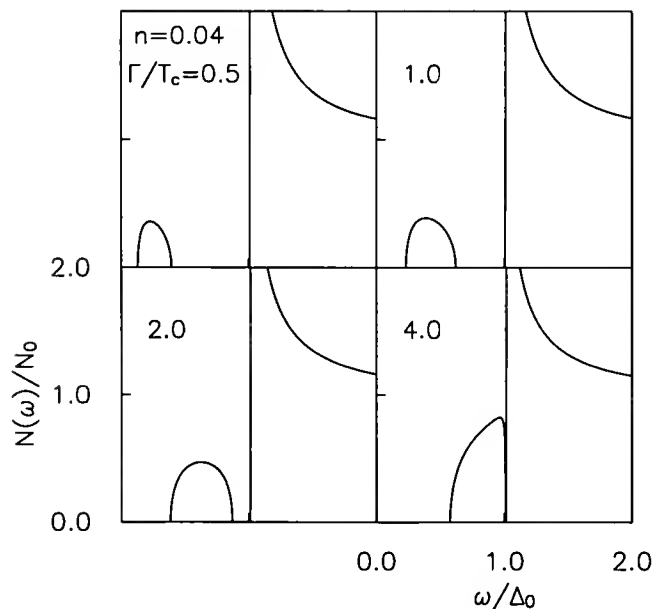**Figure 3.4** Conduction electron density of states in the Coqblin-Schrieffer limit for $N = 2$ and several values of hybridization Γ; $T_K = \Gamma$ in the CS limit. The impurity concentration is $n = 0.04$.
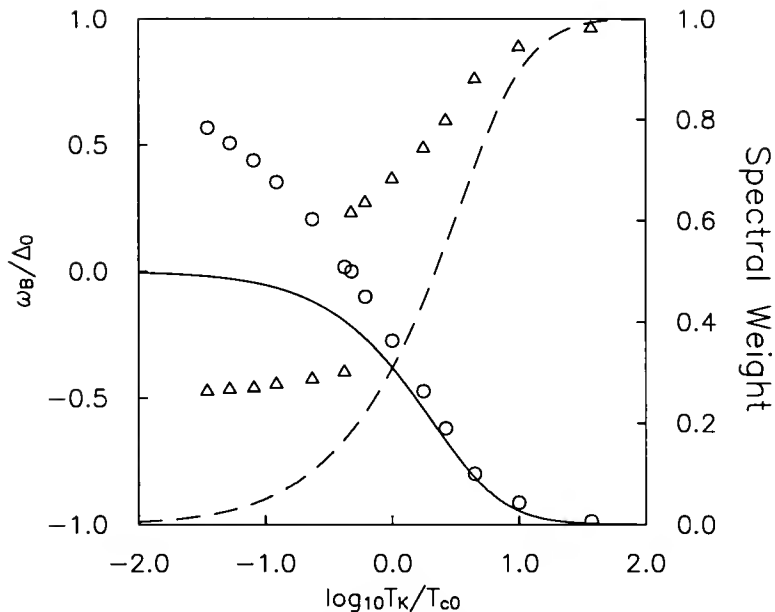
Figure 3.5 The position and spectral weight of the bound states in the gap for an s-wave superconductor with Kondo impurities. The solid (dashed) line is the location (spectral weight) of bound states. Only one of the bound states is indicated here, the other one is located at positive energies, symmetrically with respect to the gap center. Circles (triangles) refer to the position (spectral weight) obtained from an NRG calculation by Shiba et al. [52]

Monte Carlo study by Jarrell et al. [63] confirms the overall dependence of ω_B on T_K/T_c.

Bound states correspond to the poles of the T-matrix for conduction electrons, $\mathbf{T}(\omega) = V^2 \mathbf{G}_f(\omega)$ and are given by

$$|\omega| = \left(T_K{}^2 + \frac{\Gamma^2 \omega^2}{\Delta^2 - \omega^2} \right)^{1/2} - \frac{\Gamma|\omega|}{\left(\Delta^2 - \omega^2\right)^{1/2}}. \qquad (3.15)$$

We compare the solution of equation (3.15) with the NRG result in Figure 3.5 . There is a good agreement for $T_K > T_c$. For $T_K \gg T_c$ the position of bound states ω_B/Δ is a quadratic function of T_K/T_c, $|\omega_B/\Delta| \simeq 1 - 2\Delta^2/T^2{}_K$, and agrees with NRG. The discrepancy between the NRG result and our calculation for $T_K < T_c$ is not surprising since the slave-boson theory fails in the high temperature regime. The slave-boson mean-field amplitude vanishes

around $T \sim T_K$ and the theory is unable to describe the crossover to temperatures above T_K. In Figure 3.5 we also show the spectral weight of the bound states in the gap which again agree with the NRG calculation for $T_K \gg T_c$ [58].

3.2.3 Specific Heat Jump

To calculate the specific heat jump we use equations (3.4), (3.6) and (3.10), (3.11), and expand the gap equation near T_c in terms of Δ/T,

$$\ln\frac{T_{c0}}{T} = -\sum_{n\geq 0}\frac{1}{(n+1/2)(1+\alpha/B(\omega_n))} + \sum_{n\geq 0}\frac{1}{n+1/2} + \frac{1}{2}b_1\left(\frac{\Delta}{2\pi T}\right)^2, \quad (3.16)$$

where

$$b_1 = \sum_{n\geq 0}\frac{(1+2\alpha\Gamma\omega_n/B^2(\omega_n)E(\omega_n))}{(n+1/2)^3 E^3(\omega_n)}, \quad (3.17)$$

and $E(\omega_n) = 1 + \alpha/B(\omega_n)$. After expanding the free energy to fourth order in Δ we obtain

$$C_s(T_c) - C_n(T_c) = \frac{8\pi^2 N_0 T_c}{b_1}\left(1 - \sum_{n\geq 0}\frac{4\pi\alpha T_c(\omega_n+\Gamma)}{(B(\omega_n)+\alpha)^2}\right)^2. \quad (3.18)$$

As can be seen in Figure 3.6 , the dependence of $\Delta C/\Delta C_0$ on T_c/T_{c0}, for $T_K \lesssim T_{c0}$, is qualitatively different from the Fermi liquid regime. In that limit, $C^* \simeq 1 - 1/\ln(T_K/2T_{c0})$, see Figure 3.7 . Ichinose [55] and Sakurai [64] have obtained a somewhat different result, $C^* \simeq 1 - 1/\ln^2(T_K/T_{c0})$.
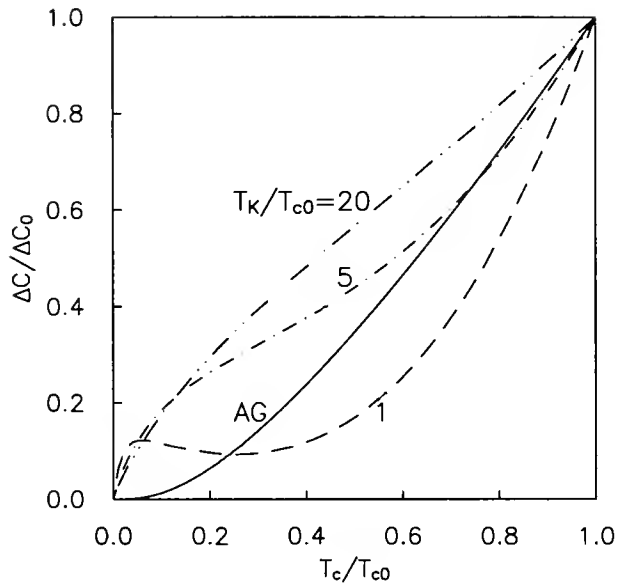
Figure 3.6 Specific heat jump as a function of T_c/T_{c0}. The result of the Abrikosov-Gor'kov theory is included for comparison.
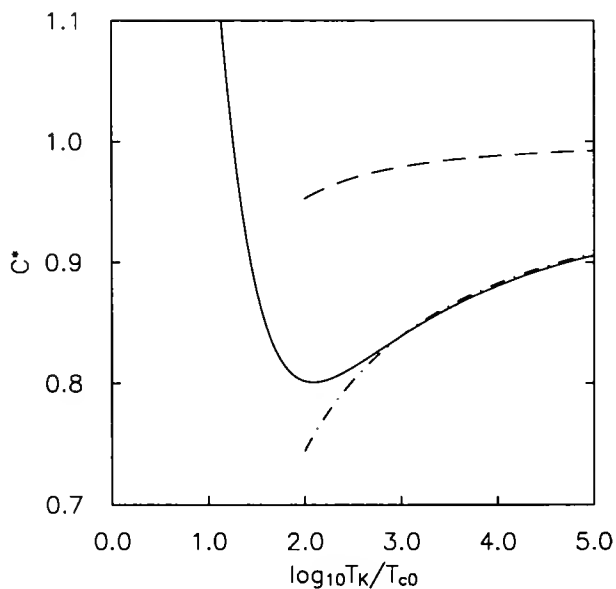
Figure 3.7 The derivative of the specific heat jump evaluated at zero impurity concentration as a function of T_K/T_c for an s-wave superconductor. The dash-dotted line shows the asymptotic behavior, $1 - 1/\ln(T_K/2T_{c0})$. The dashed line is the asymptotic form at $T_K/T_c \to \infty$ found in Refs. [49] and [58], $C^* \simeq 1 - 1/\ln^2(T_K/T_{c0})$.

3.2.4 Penetration Depth

If an electromagnetic wave of frequency ω is normally incident on plane superconducting surface, the current response may be written $\mathbf{j}(\mathbf{q}, \Omega) = -\overleftrightarrow{K}(\mathbf{q}, \Omega)\mathbf{A}(\mathbf{q}, \Omega)$, where $\mathbf{A}$ is the applied vector potential. The penetration depth, $\lambda = \left[-\frac{4\pi}{c} K(0,0) \right]^{-1/2}$, can be calculated following the derivation of Skalski et al. [65],

$$
\lambda = \left(\frac{mc^2}{4\pi e^2} \right) \left(\frac{\Delta}{2\pi T} \right)^{1/2}
$$
$$
\times \left[\sum_{n \geq 0} \frac{1}{((1 + (\tilde{\omega}_n/\tilde{\Delta})^2)^{1/2} + \alpha\Gamma/\Delta A)(1 + (\tilde{\omega}_n/\tilde{\Delta})^2)} \right]^{-1/2} \qquad (3.19)
$$

where $A = \omega_n^2 + T_K^2 + 2\omega_n\Gamma\tilde{\omega}_n/\sqrt{\tilde{\Delta}^2 + \tilde{\omega}_n^2}$. The zero temperature penetration depth is given in the strong coupling limit by

$$
\frac{\lambda(0)}{\lambda_L(0)} \simeq 1 + \frac{\alpha}{2T_K^2} \left(1 + \frac{\pi\Gamma}{4\Delta} \right) \simeq \frac{N}{16} \frac{T_{c0}}{\Delta_0} \frac{\Gamma^2}{T_K^2}, \qquad (3.20)
$$

which for $N = 2$ is equal to 1.071 in the Coqblin-Schrieffer limit. A numerical calculation of the penetration depth shows that the derivative $\partial(\lambda(0)/\lambda_L(0))/\partial\bar{n}$, evaluated at $\bar{n} = 0$, is a weakly varying function of T_K/T_{c0} for $1 \lesssim T_K/T_{c0} < \infty$. The penetration depth is much less affected by impurity doping on the high temperature side, where $\partial(\lambda(0)/\lambda_L(0))/\partial\bar{n}_{|n=0}$ reaches values much smaller than those in the strong coupling regime. We now see that the superfluid density at $T = 0$ does not scale with the T_c suppression in the Fermi liquid regime. While the slope of the initial T_c suppression goes to 0 in the limit $T_K/T_{c0} \to \infty$, the slope of the initial increase of the $T = 0$ penetration depth remains large.

3.3 Unconventional Superconductors

The problem of an Anderson impurity in an unconventional superconductor is of considerable interest for several reasons. First, it serves as a testing ground for the ideas of Withoff and Fradkin, who argued that in the analogous Kondo problem with power law conduction electron density of states, $N(\omega) = C|\omega|^r$, there existed a critical coupling below which impurities are effectively decoupled from the conduction band [3, 66]. We showed in the preceding chapter that in an unconventional superconductor a critical coupling indeed exists for the 1-impurity problem, but that for a finite density of impurities there is always a finite density of conduction electron states at the Fermi level, provided $N = 2$ or if $r \leq 1$. This is consistent with phenomenological studies of potential scattering in unconventional superconductors [5,6]. This does not exclude the possibility of observing some vestige of this transition as the Kondo temperature becomes quite small, however. Secondly, Kondo impurities in unconventional superconductors have been proposed as analogues of defects in Kondo lattices [67], with the argument that a vacancy in a Kondo lattice may induce a *relative* phase shift close to $\pi/2$.

We chose to do our calculations for the axial, $\Delta(k) = \Delta_0(\hat{k}_x + i\hat{k}_y)$, and polar, $\Delta(k) = \Delta_0\hat{k}_z$, states for simplicity. These two states, nominally p-wave pairing states over a spherical Fermi surface in 3D, are quite generally representative of two classes of order parameters. States with order parameters vanishing at points on the Fermi surface, like the axial state, have low temperature properties associated with a quasiparticle density of states $N(\omega) \sim \omega^2$, whereas the states with lines of nodes, like the polar state, correspond to $N(\omega) \sim \omega$. More complicated order parameters, such as those having a *d*-wave

symmetry, will have similar properties at low temperatures, since the main factor determining the low-T properties is the order parameter topology, i.e. whether there are points or lines of zeros of the order parameter. In the case of points (lines) of nodes, the low-temperature specific heat of pure supercon- ductors is proportional to T^2 (T). The deviation of the penetration depth $\Delta\lambda$ from its zero temperature value $\lambda(0)$ along the main axes of symmetry of the order parameter is either $\sim T^2$ or $\sim T^4$ in the axial state, according to the direction of current flow [68], whereas for the polar state it is either $\sim T$ or $\sim T^3$. The presence of strong impurity scattering complicates the picture and these power laws do not hold in general.

3.3.1 Suppression of the Critical Temperature

Due to the absence of the Anderson theorem for p-wave-like or d-wave-like superconductors, the influence of impurity scattering on the critical tempera- ture is qualitatively different from that of s-wave-like superconductors [4, 69]. For the unconventional states of interest, there are no off-diagonal corrections to the superconducting Green's function, $\tilde{\Delta} = \Delta$.

In this case T_c for either type of state is determined by

$$\ln(T_c/T_{c0}) = 2\pi T_c \sum_{n\geq 0} \frac{1}{\omega_n(1 + \alpha/B(\omega_n)) + \alpha/B(\omega_n)} - \sum_{n\geq 0} \frac{1}{n + 1/2}. \quad (3.21)$$

The initial T_c-suppression is then given by

$$\left(\frac{1}{T_{c0}}\frac{dT_c}{d\bar{n}}\right)_{n=0} = -\frac{N}{4\pi^2} \sum_{n\geq 0} \frac{\Gamma(\omega_n + \Gamma)}{(n + 1/2)^2 B(\omega_n)}, \quad (3.22)$$

and approaches $-N\Gamma^2/8T_K^2$, in the limit $T_K/T_{c0} \to \infty$, see Figure 3.8 . Note that $\tilde{\omega}_n/\Delta \to \alpha\Gamma/\Delta T_K^2$, as $T_c \to 0$, and as a consequence the critical concen- tration n_c is finite.
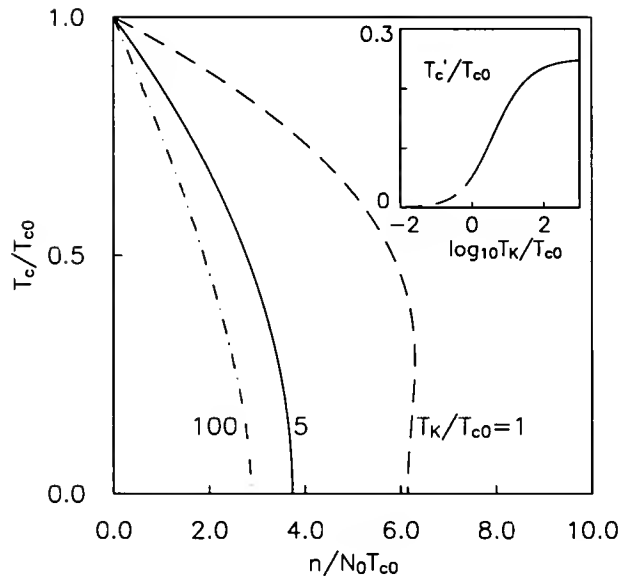
Figure 3.8 Critical temperature vs. impurity concentration for unconventional states considered in this work. The initial slope at T_{c0} is shown in the inset.

3.3.2 Density of States

The effect of Kondo impurities on the density of states is shown in Figures 3.9 and 3.10 . As in the s-wave case, the resonant states move towards the edges of the gap as T_K/T_c increases, except in the special case $N = 2$, where they are pinned at the gap center. In all cases the impurity bands are broadened relative to the s-wave case by the continuum in which they are embedded. In the limit $T_K \to \infty$, the current theory coincides with the results given by phenomenological T-matrix treatments [5,6] for $N = 2$.

3.3.3 Specific Heat

To obtain the specific heat we differentiate the entropy with respect to temperature $C_v = TdS/dT$. The entropy of conduction electron quasiparticles renormalized by impurities is given by
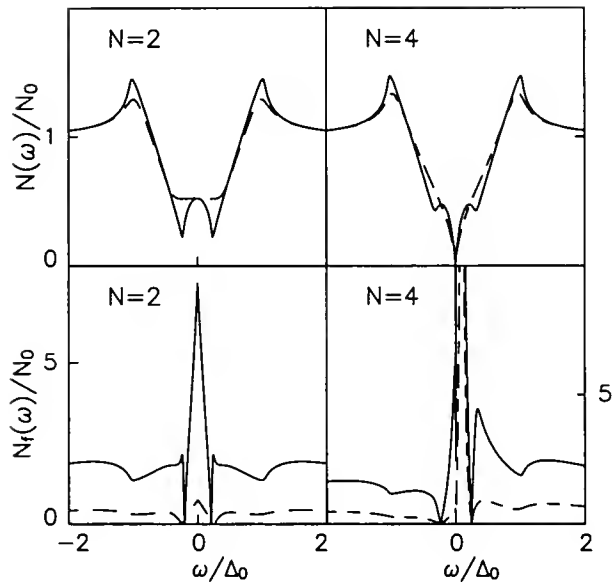
Figure   3.9 Conduction electron and impurity spectral functions in the Kondo limit in a polar state for $N = 2$ and $N = 4$. The solid and dashed lines correspond to $T_K = T_c$, and $T_K = 10T_c$, respectively. The concentration of impurities is $\bar{n} = 0.4$.

$$S = -k_B \int_0^\infty d\omega N(\omega)[f\ln f + (1 - f)\ln(1 - f)], \tag{3.23}$$

where $f = f(\omega)$ is the Fermi function. Note that the density of states $N(\omega)$ is calculated self-consistently, using equations (3.2), (3.3), and (2.20).

The presence of resonances at low energies leads to pronounced features in the low–T specific heat, as shown in Figure 3.11 . For $T_K \gg T_c$, $N = 2$, these features are identical to those predicted by the phenomenological theory of Refs.   [5,6, 70]. For smaller T_K/T_c, the resonance sharpens, as is evident from, e.g., Figure 3.10 . In this case resonances in the low-temperature specific heat may be quite dramatic. Figure 3.12 shows the temperature dependence of C/T for $N = 2$ in the axial state for the case when the resonance is very narrow,
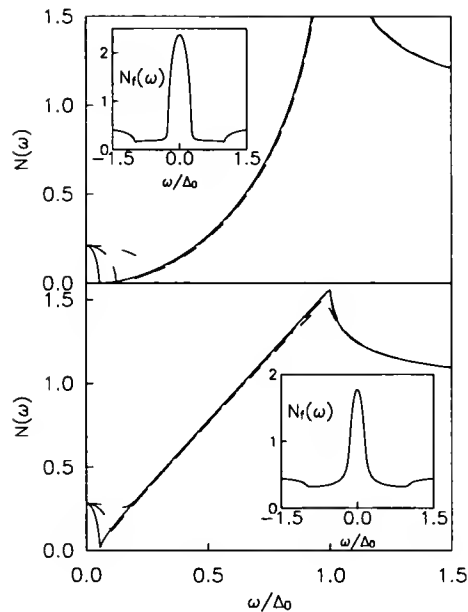
Figure 3.10 Density of states for conduction electrons in axial (at top) and polar (at bottom) state for $N = 2$ and $T_K/T_{c0} = 0.3$ (solid line), 1 (dashed line), and 20 (dash-dotted line). The inset shows the impurity spectrum for $T_K/T_{c0} = 20$ in both states. The scaled impurity concentration is $\bar{n} = 0.2$.

$\Gamma \ll T_c$ and just above the Fermi surface, $\epsilon_f \ll T_c$. Such pronounced features are possible only when the bare impurity level is close to the Fermi surface, and the hybridization is weak. They will be sharper for superconducting states with larger exponent r in the unperturbed density of states $N(\omega) \simeq C|\omega|^r$ at low ω. These anomalies may be observed experimentally at sufficiently low temperatures. In this context, it is interesting to note that a sharp peak in C/T has been observed in the heavy fermion superconductor UPt_3 at 18 mK [71]. This peak is present at roughly the same position also in the normal state at magnetic fields $B \geq B_{c2}$, as might be expected in a situation where the Kondo temperature is significantly smaller than the critical temperature. If such an interpretation of the measurement of Schuberth et al. in these terms is correct, we would expect the size of the peak to scale with other measures
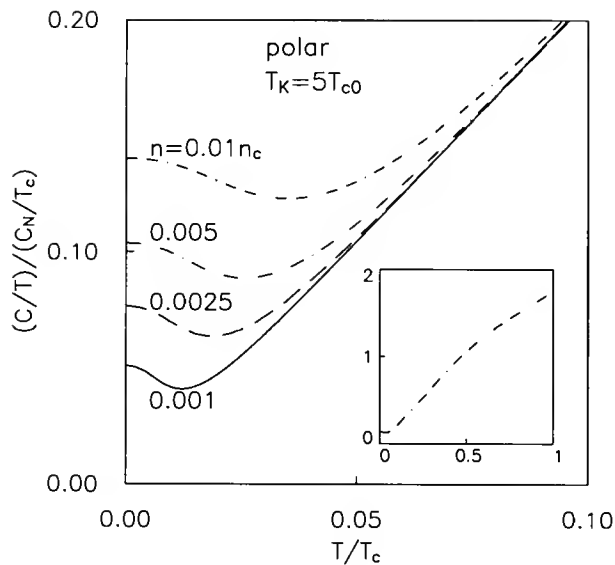
Figure 3.11 The low-T part of C/T in the polar state for $N = 2$ in the Kondo limit. The inset shows C/T for $n = 0.01 n_c$ over the full temperature range.

of the defect concentration, such as T_c the size of the specific heat jump, in different samples. We note, however, that fields of order 1 Tesla would normally destroy a many-body resonance of the usual magnetic type.

3.3.4 Specific Heat Jump

The specific heat jump at T_c can be found by the method already mentioned in the preceding section,

$$
C_s(T_c) - C_n(T_c) = \frac{8\pi^2 N_0 T_c}{b_1} \left[1 - \sum_{n \geq 0} \left(\frac{G(\omega_n)}{((n + 1/2)E(\omega_n) + \alpha/B(\omega_n))^2} \right) \right]^2,
$$
(3.24)
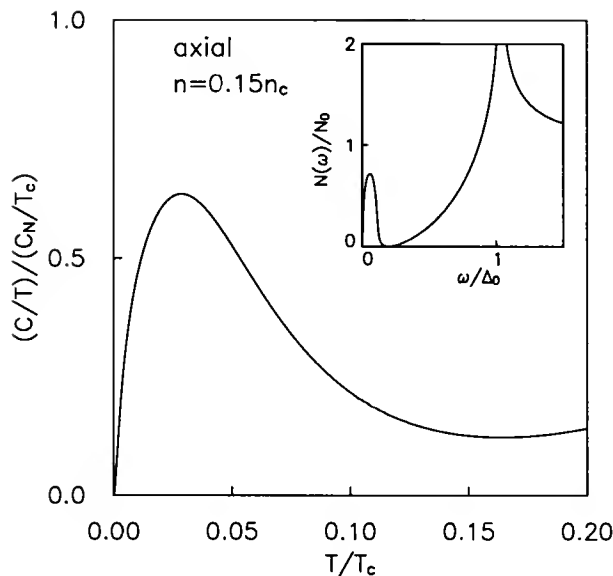
Figure 3.12 The low-T part of C/T in the axial state. Note the sharp resonance in the density of states at low energies (the inset).

where

$$b_1 = \sum_{n \geq 0} \frac{b + cH(\omega_n)}{[(n + 1/2)E(\omega_n) + \alpha/B(\omega_n)]^3}, \qquad (3.25)$$

with $b = 4/5$ $(3/5)$, and $c = 2/3$ $(1/3)$, for the axial (polar) state, and

$H(\omega_n) = \alpha\Gamma \left[2(\omega_n + \Gamma)^2/B(\omega_n) - 1\right]/B(\omega_n)$, $G(\omega_n) = 2\alpha\omega_n(\omega_n + \Gamma)(n +$

$1/2 + \Gamma/2\pi T_c)/B^2(\omega_n) + \alpha\Gamma/2\pi T_c B(\omega_n)$.

The derivative of the specific heat jump, C^*, is shown in Figure 3.13 .

3.3.5 Penetration Depth

We now discuss the low-temperature response functions of the supercon-

ductor in the presence of Kondo impurities, which have not to our knowledge

been previously calculated in the strongly interacting Fermi liquid regime of

interest. The effect of Kondo impurities on the electromagnetic response has
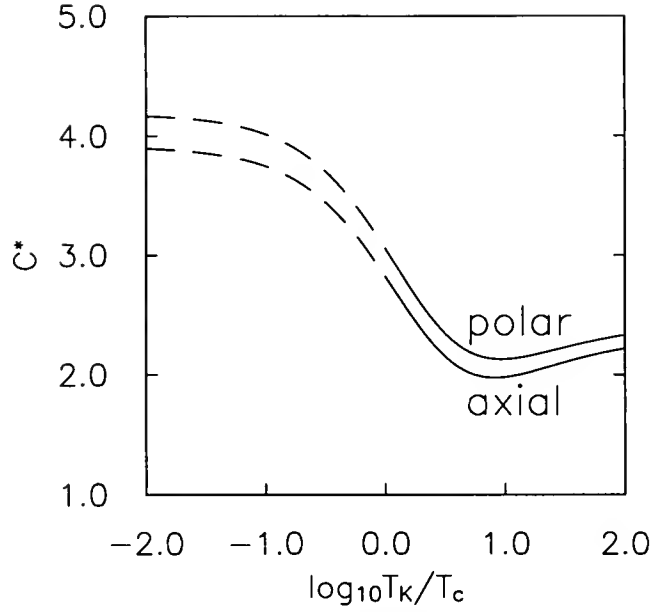
Figure 3.13 The derivative of the specific heat jump evaluated at zero impurity concentration as a function of T_K/T_c for the axial and polar superconducting states.

been calculated in the phenomenological T-matrix approach mentioned above, and used to analyze experiments on heavy fermion and high–T_c superconductors with impurities, but no microscopic theory is available. The London penetration depth is obtained from $\lambda = \left[-\frac{4\pi}{c} K(0,0) \right]^{-1/2}$, where $K(0,0)$ is the electromagnetic response kernel. The kernel is given by the linear response formula

$$K^{ij}(0,\Omega_m) = -\frac{3e^2 T}{2mc} \int_{-\infty}^{\infty} d\epsilon \sum_n \mathrm{Tr}\langle \hat{k}_i \hat{k}_j \mathbf{G}(k,\omega_n)\mathbf{G}(k,\omega_n - \Omega_m)\rangle_{\hat{k}}. \quad (3.26)$$

In the static limit, $\Omega_m \to 0$, the kernel becomes

$$K^{ij}(0,0) = -\frac{6\pi e^2 T}{mc} \sum_n \int \frac{d\Omega}{4\pi} \hat{k}_i \hat{k}_j \frac{\Delta^2(k)}{(\Delta^2(k) + \tilde{\omega}_n^2)^{3/2}}, \quad (3.27)$$
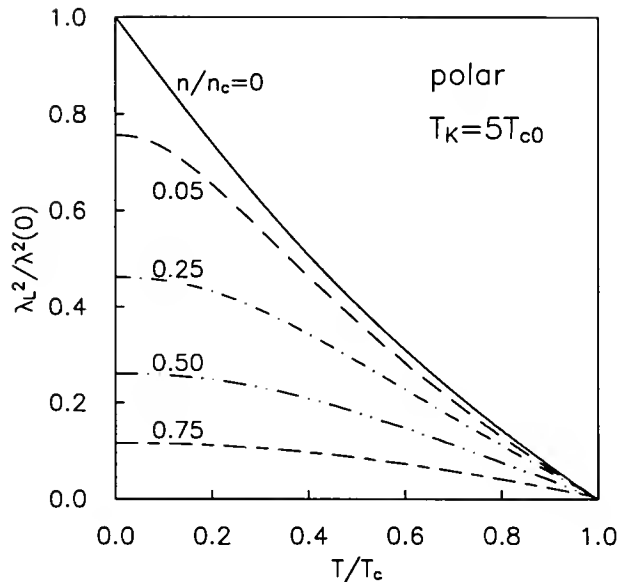
Figure 3.14 The inverse square of the penetration depth vs. temperature at several concentrations of impurities in the polar state.

where the integral represents the angular average.

Here we specialize again to the $N = 2$ case. The temperature dependence of $(\lambda^{11})^{-2}$ in the polar state, which corresponds to the component of the superfluid density within the plane containing the line of zeroes of the order parameter, is shown in Figure 3.14 . The low-T behavior changes from linear to quadratic upon doping. A similar result was obtained earlier [68, 72] within the phenomenological theories. The results for $T_k \simeq T_c$ are qualitatively very similar to those shown. Finally, λ^{-2} at $T = 0$ along the main axes of symmetry for the axial and the polar state as a function of impurity concentration is presented in Figure 3.15 . We note that the largest component of the penetration depth scales in the case of line nodes as $\lambda(n)/\lambda_L(0) - 1 \sim n^{1/2}$ at low concentrations [73], and $\lambda^{-2}(n) \sim \log(n_c/n)$ close to the critical concentration.
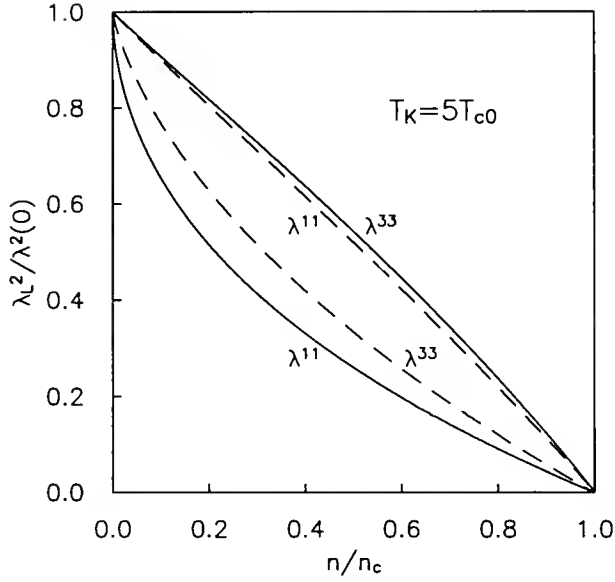
Figure 3.15 The inverse square of the $T = 0$ penetration depth in the two principal directions as a function of impurity concentration for the polar (full lines) and the axial state (dashed lines).

Similar suppression of the superfluid density was calculated for a d-wave order parameter within a phenomenological model in Ref. [74]. It is clear that both the concentration and temperature dependence of the penetration depth components may be important tests of gap anisotropy.

CHAPTER 4
ANISOTROPIC CONVENTIONAL SUPERCONDUCTORS VS. UNCONVENTIONAL SUPERCONDUCTORS

4.1 <u>Experimental Motivation</u>

Recent high resolution angle-resolved photoemission (ARPES) experiments on Bi-2212 have been interpreted in terms of a highly anisotropic order parameter with a large gap in the $(\pi, 0)$ direction and two lines of nodes near a small gap in the (π, π) direction [75, 76].
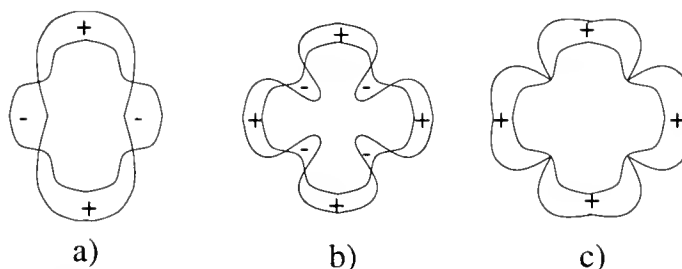
Figure 4.1 Order parameters plotted over tetragonal Fermi surface: a) $d_{x^2-y^2}$ state. b) extended s-wave state; c) s-wave state with gap minima at Fermi surface.

While alternative explanations consistent with an order parameter Δ_k which reduces the symmetry of the Fermi surface (e.g. d-wave, see Figure 4.1 a) have been put forward [77], it is interesting to consider the consequences of the simpler suggestion that Δ_k has the full symmetry of the crystal, but changes sign (see Figure 4.1 b). Fehrenbacher and Norman [78] have considered the effects of potential scattering on such a state, following earlier work

48

on anisotropic-s states with nodes [79], and shown that small concentrations of impurities can lead to "gapless" behavior in the density of states (i.e., with residual density of states $N(0) > 0$), followed by the opening of an actual induced gap in the quasiparticle spectrum as the concentration is increased further.

The prediction of a range of impurity concentrations over which "gapless" behavior is predicted is important because microwave and NMR experiments, particularly on Zn and Ni-doped YBCO crystals [80, 81, 82, 83] have shown evidence of low-temperature thermodynamic properties reflecting the existence of a residual density of states. They have been interpreted most often in terms of a d-wave pairing scenario [73, 84, 85, 86, 87], where the well-known effect of dirt is to induce a residual density of states for infinitesimal concentrations [69]. The intriguing possibility raised by the ARPES experiment [75,76] is that many of the observations of "gapless" behavior can be equally well explained by an anisotropic state with extended-s symmetry. There are some difficulties associated with this interpretation even if it can successfully account for the microwave and NMR data. The most important of these is the set of SQUID experiments [12,13,14,15] indicating that the order parameter Δ_k changes sign under a $\pi/2$ rotation. While the extended-s order parameter discussed here indeed changes sign over the Fermi surface, the symmetry of the expected tunneling currents is not, within the simplest theory, consistent with the observations reported [88, 89]. Furthermore, the existence of a small gap in the (π, π) direction in BSCCO has been questioned by at least one other photoemission group claiming similar angular and energy resolution [90]. We do not address any of these discrepancies in this work.
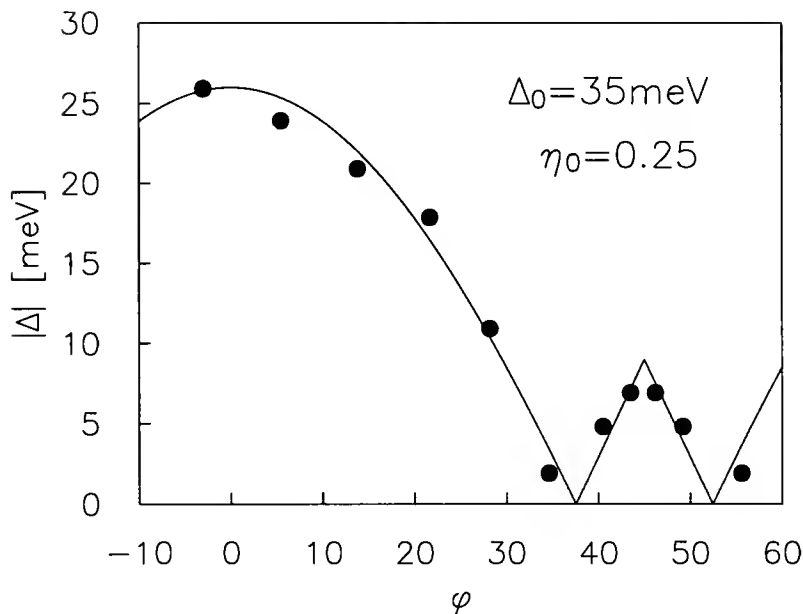
Figure 4.2 ARPES determination of BSCCO energy gap as function of angle ϕ around Fermi surface. Data from Ref. 1. Solid line: $\Delta_k = \Delta_0(|\cos 2\phi| - \eta_0)$, with $\eta_0 = 0.25$.

4.2 The Model

In the absence of definitive answers to the above questions, we assume the plausibility of the Argonne-U. Illinois argument and investigate the consequences of assuming the order parameter symmetry identified in Refs. [75,76] within a generalized BCS model.

While these authors pointed out that their data were consistent with an order parameter over a realistic BSCCO Fermi surface with symmetry $\Delta_k \sim \cos k_x \cos k_y$, we work here with an even simpler model with cylindrical Fermi surface, in which case a rather good fit to the data can be obtained by assuming $\Delta_k = \Delta_0(|\cos 2\phi| - \eta_0)$, with Δ_0=35meV and $\eta_0 = 0.25$, as shown in Figure 4.2 . With this set of parameters, a BCS weak-coupling approach yields the gap magnitude ratio $\Delta_0/T_c = 2.92$, see Figure 4.3 .
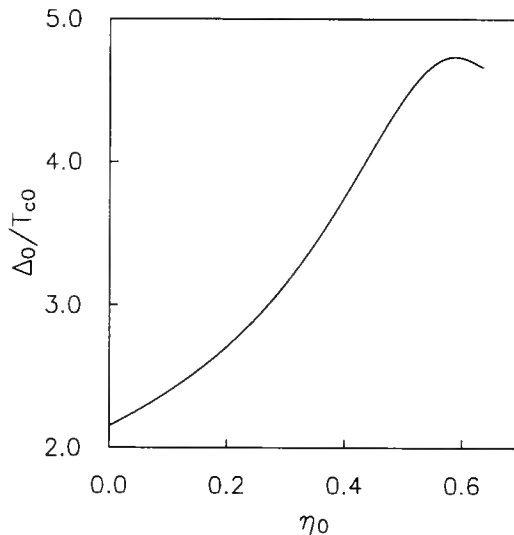
Figure 4.3 The ratio Δ_0/T_{c0} as a function of η_0.

Note that η_0 controls the angular range over which the s-wave order parameter is negative. The case $\eta_0 = 0$ corresponds to a somewhat pathological state of type c), while $\eta_0 = 2/\pi$ corresponds to equal positive and negative weights, $\langle \Delta_k \rangle = 0$, where $\langle ... \rangle$ is a Fermi surface average. When $\eta_0 = 0$, the energy of quasiparticle excitations is identical to that of the d-wave state $d_{x^2-y^2}$. Other choices of basis functions may result in a somewhat better overall fit and avoid the cusp at $\phi = \pi/4$, but we do not expect these details to affect our qualitative conclusions.

Measurements of penetration depth, angle-resolved photoemission, thermal conductivity, and nuclear magnetic relaxation experiments provide evidence for gap nodes, but do not determine if the order parameter changes sign. This is because experiments of this kind are normally assumed to measure properties sensitive to the order parameter Δ_k only through the Bogoliubov quasiparticle spectrum, $E_k = \sqrt{\xi_k^2 + |\Delta_k|^2}$. Since E_k does not depend on the sign of the order parameter, all three states shown in Figure 4.1 have similar (linear)
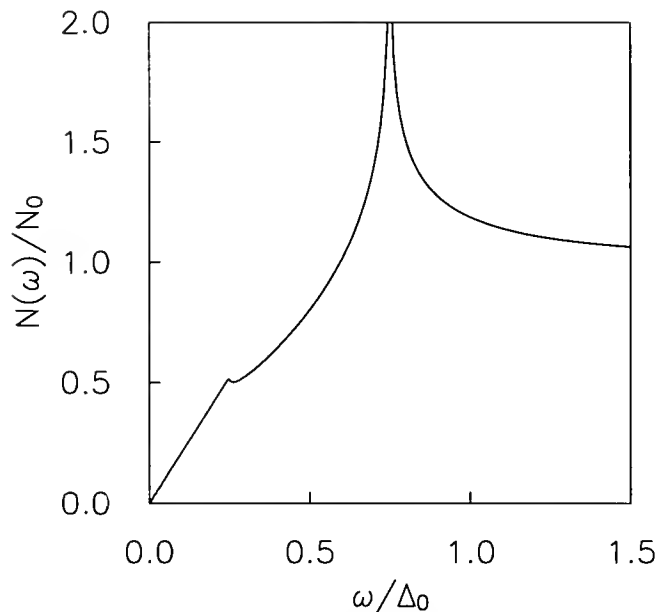
Figure 4.4 Density of states for the superconducting state with an extended-s order parameter, $\Delta_k = \Delta_0(|\cos 2\phi| - \eta_0)$, with $\eta_0 = 0.25$.

low-energy density of single-particle states $N(\omega)$, and all properties deriving directly therefrom.

Figure 4.4 shows density of states for the state of the type 4.1 c. Note the low-energy gap feature corresponding to the smaller gap maximum.

Systematic impurity-doping studies of transport properties can in principle help to identify the order parameter symmetry, however. Unconventional states like the $d_{x^2-y^2}$ state (Figure 4.1 a) possess nodes on the Fermi surface for symmetry reasons, whereas their existence is "accidental" in the s-wave case (Figure 4.1 b-c). In the d-wave case, supression of gap variation in k-space can only result in an overall supression of the order parameter magnitude, whereas in s-wave cases b) and c), it results eventually in the elimination of the nodes. In many-body language, the crucial point is that the off-diagonal impurity self-energy Σ_1 is nonzero in s-wave states 4.1 a and 4.1 b, but vanishes in the d-wave state 4.1 c. In the isotropic s-wave state, a large Σ_1 cancels the diagonal

self-energy Σ_0 [1], leading to Anderson's theorem [2], whereas in extended-s states this cancellation is only partial. A large Σ_1 furthermore prevents the formation of a scattering resonance at the Fermi surface, leading to clean limit low-frequency transport coefficients which in extended-s states for $T \ll T_c$ vary relatively weakly with temperature. By contrast, in the d-wave (or other unconventional state where $\Sigma_1 = 0$), resonant scattering leads to transport properties which vary strongly in temperature for $T \ll T_c$ [91,5,6]. In this sense the characteristics attributed to extended-s states here are also valid qualitatively for any mechanism which generates an off-diagonal self-energy in a d-wave state as well, e.g. tetragonal symmetry breaking or locally induced s-wave components due to impurity potentials.

The disorder-averaged matrix propagator describing any of the states a)-c) above is written

$$g(\vec{k}, \omega_n) = \frac{\tilde{\omega}\underline{\tau}^0 + \tilde{\xi}_k\underline{\tau}^3 + \tilde{\Delta}_k\underline{\tau}^1}{\tilde{\omega}^2 - \tilde{\xi}_k^2 - |\tilde{\Delta}_k|^2} \tag{4.1}$$

where the $\underline{\tau}^i$ are the Pauli matrices and $\tilde{\Delta}_k$ is a renormalized unitary order parameter in particle-hole and spin space. The renormalized quantities are given by $\tilde{\omega} = \omega - \Sigma_0(\omega)$, $\tilde{\xi}_k = \xi_k + \Sigma_3(\omega)$, and $\tilde{\Delta}_k = \Delta_k + \Sigma_1(\omega)$, where the self-energy due to s-wave impurity scattering has been expanded $\underline{\Sigma} = \Sigma_i\underline{\tau}^i$. The relevant self-energies are given in a self-consistent t-matrix approximation [5,6] by

$$\Sigma_0 = \frac{\Gamma G_0}{c^2 + G_1{}^2 - G_0{}^2}; \ \Sigma_1 = \frac{-\Gamma G_1}{c^2 + G_1{}^2 - G_0{}^2}, \tag{4.2}$$

where $\Gamma \equiv n_i n/(\pi N_0)$ is a scattering rate depending only on the concentration of defects n_i, the electron density n, and the density of states at the Fermi level, N_0, and we have defined $G_\alpha \equiv (i/2\pi N_0)\Sigma_k Tr[\underline{\tau}^\alpha g]$. The strength of an individual scattering event is characterized by the cotangent of the scattering

phase shift, c. The Born limit corresponds to $c \gg 1$, so that $\Sigma_{0_1} \simeq \pm \Gamma_N G_{0_1}$, while the unitarity limit corresponds to $c = 0$. We have defined the normal-state impurity scattering rate as $\Gamma_N \equiv \Gamma/(1 + c^2)$; note that in the high-$T_c$ cuprates the total scattering rate at T_c includes inelastic scattering and is expected to be much larger for clean samples.

4.3 Density of States

A crucial feature of the physics of d-wave superconductors is that an infinitesimal concentration of impurities produces a finite density of states $N(0) > 0$ at the Fermi level [69], leading to temperature dependences characteristic of the normal state in all transport quantities. Solving the self-consistency equations at $\omega = 0$ for the extended-s wave state under consideration leads immediately to the conclusion that such "gapless" behavior is possible only for a range of scattering rates $\Gamma < \Gamma_c$, however [78].

This is illustrated in Figure 4.5 . A low frequency expansion in the gapless regime yields $\Gamma_c/T_{c0} \simeq \eta_0(1 + c^2)$.

Can the same experiments which seem to fit the "dirty d-wave" scenario also be explained by extended-s states? The difficulty is how to fix the actual impurity scattering rate, Γ, given the known concentration. One way is to attribute the additional extrapolated $T \to 0$ resistivity to impurity scattering, such that the elastic and inelastic rates add incoherently. If one attempts such an analysis for Zn-doped YBCO crystals using results from, e.g., Chien et al. [92], one finds that $\Gamma/T_c \simeq 0.3 - 0.5$ per 1% Zn. Since Zn doping studies of YBCO indicate gapless behavior up to several per cent Zn, it would appear that an extended-s picture is plausible for YBCO only if one assumes η_0 close to the critical value $2/\pi$ for which $\langle \Delta_k \rangle = 0$. We are not aware of similar
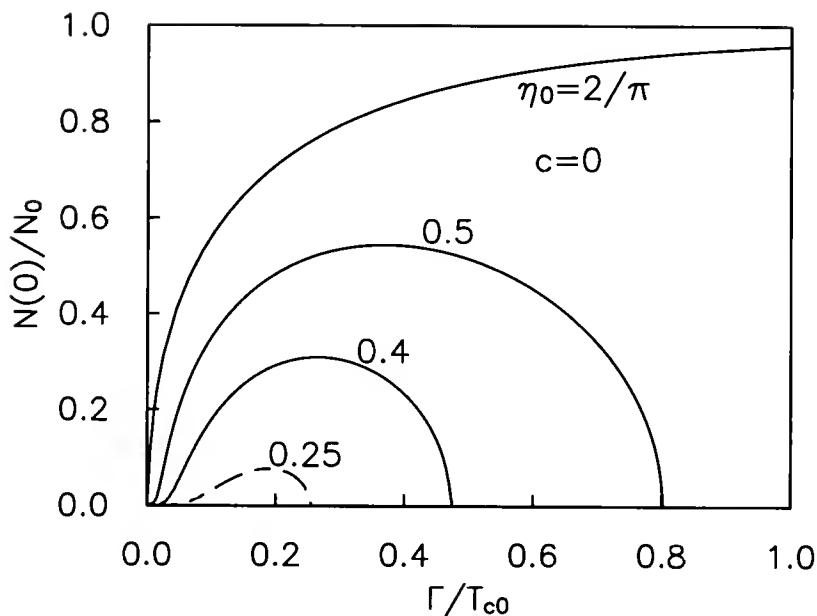
Figure 4.5 Residual density of states $N(0)/N_0$ in extended-s state vs. normalized scattering rate Γ/T_{c0} for $c = 0$. Dashed line: $\eta_0 = 0.25$ obtained from fit to data of Ding et al.

doping studies in single crystal BSCCO, but assuming for the moment that Zn scatters equally strongly in this material, we see from the dashed line in Figure 4.5 that a well-developed gap Ω_G in the excitation spectrum should be induced in BSCCO by a few per cent Zn doping. Note that the results shown in Figure 4.5 are not sensitive to changes in the scattering phase shift δ_0. In the special case, $\eta_0 = 0$, a simple estimate shows that for small scattering rates, $\Omega_G \sim \Gamma$ (Γ_N in Born limit).

In the dirty limit $\Gamma \to \infty$, the s-wave superconductor becomes isotropic with a BCS density of states $N(\omega) = \mathrm{Re}\, \omega/\sqrt{\omega^2 - \Delta_{avg}^2}$, as shown in Figure 4.6 . In contrast to a d-wave superconductor, the self-energies obtained in the Born approximation and in the resonant scattering limit are almost equivalent in the highly anisotropic s-wave system, if $\eta_0 \ll \Delta_{avg}/\Delta_0$. This insensitivity to larger phase shifts arises because of off-diagonal self-energy corrections which
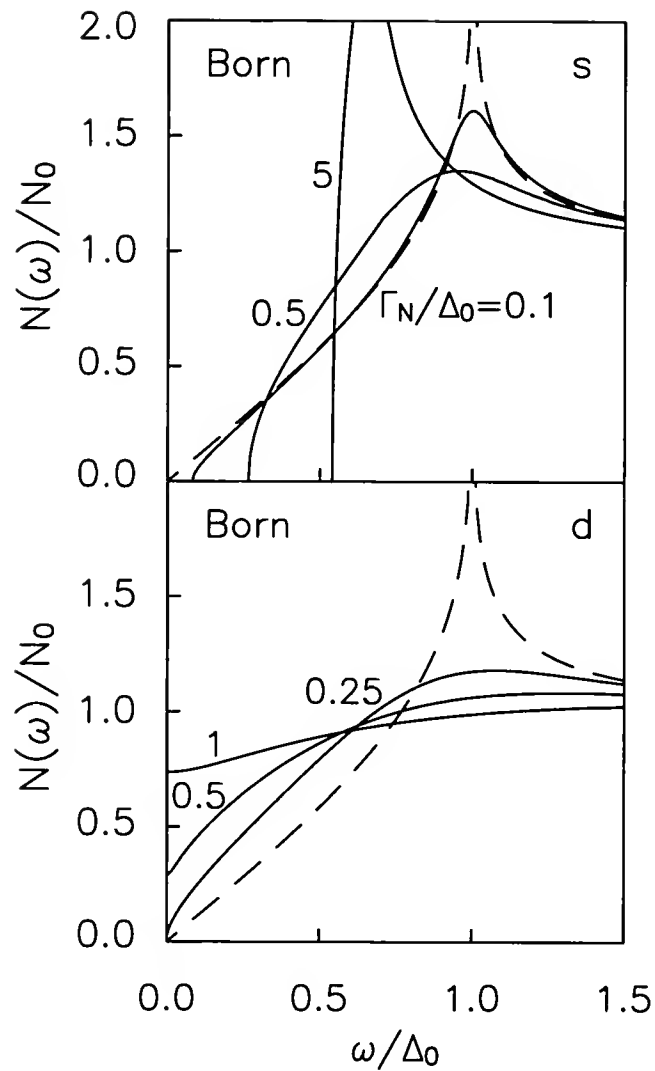
Figure 4.6 Normalized density of states $N(\omega)/N_0$ for s– and d–wave order parameters vs. reduced frequency ω/Δ_0, shown for various potential scattering rates Γ_N/Δ_0 in the Born approximation; $\eta_0 = 0$.

prevent the occurence of poles in the t-matrix, $c^2 - G_0{}^2 + G_1{}^2 \simeq \mathcal{O}(1)$ for all $c \lesssim 1$. Densities of states for both types of states in the limit of resonant scattering are shown in Figure 4.7 .
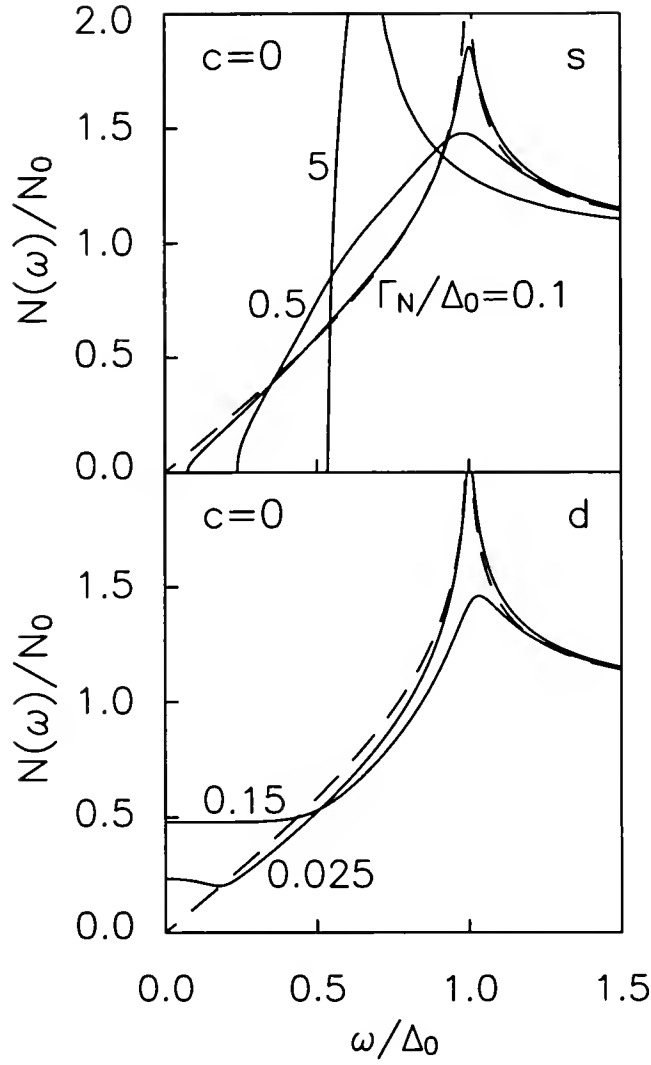
Figure 4.7 Normalized density of states $N(\omega)/N_0$ for s– and d–wave order parameters vs. reduced frequency ω/Δ_0, shown for various potential scattering rates Γ/Δ_0 in the unitarity limit, $c = 0$; $\eta_0 = 0$.

4.4 Critical Temperature

We first solve the Dyson equation for the renormalized propagator (4.1) together with the gap equation. The order parameter Δ_k is related as usual to the off-diagonal propagator as $\Delta(k) = T \sum_n \sum_{k'} V_{kk'} \text{Tr}(\tau_1/2)\underline{g}(k', \omega_n)$, where $V_{kk'} \equiv V_{d,s}\Phi_{d,s}(\hat{k})\Phi_{d,s}(\hat{k}')$ is the phenomenological pair interaction assumed.

In the d-wave case, $\Delta_k = \Delta_0{}^d \Phi_d(\hat{k})$, with $\Phi_d = \cos 2\phi$, yielding a simple equation for the gap maximum $\Delta_0{}^d$,

$$\lambda_d{}^{-1} = \left\langle \int_0^{\omega_D} d\omega \tanh \frac{\beta\omega}{2} \, \text{Re} \frac{\Phi_d^2}{\sqrt{\tilde{\omega}^2 - \Delta_k{}^2}} \right\rangle, \tag{4.3}$$

where $\lambda_d = V_d N_0$, and $\langle ... \rangle$ represents an angular average over the cylindrical Fermi surface. In the s-wave case, on the other hand, it is convenient to put $\Delta_k = \Delta_{avg} + \Delta_{1k}$, where $\Delta_{avg} = \langle \Delta_k \rangle$ is the gap average over the Fermi surface. When impurities are added to the system, it is easy to check that $\tilde{\Delta}_k = \tilde{\Delta}_{avg} + \Delta_{1k}$, determined by

$$\lambda_s{}^{-1} = \left\langle \int_0^{\omega_D} d\omega \tanh \frac{\beta\omega}{2} \, \text{Re} \frac{\Phi_s \tilde{\Delta}_k / \Delta_0}{\sqrt{\tilde{\omega}^2 - \tilde{\Delta}_k^2}} \right\rangle. \tag{4.4}$$

Note this is effectively an equation for $\tilde{\Delta}_{avg}(\omega)$ since the angular variation Δ_{1k} is given. When $\eta_0 = 0$ the initial slope of T_c suppression, $dT_c/d\Gamma_N = -\chi \pi/4$, where $\chi \equiv [\langle \Phi_s^2 \rangle - \langle \Phi_s \rangle^2]/\langle \Phi_s \rangle^2$ is $1 - 8/\pi^2$ for the s-wave and 1 for the d-wave state considered. In the d-wave case the critical temperature continues to drop rapidly to zero at a critical concentration of $n_i^c = \pi^2 N_0 T_{c0}/2e^\gamma$, whereas the decrease becomes more gradual as the gap is smeared out in the s-wave case, finally varying [93, 94, 95] as $T_c \sim T_{c0}[1 - \chi \ln(1.154\Gamma_N/\pi T_{c0})]$.

The initial suppression of T_c depends also on the magnitude of η_0 and the magnitude of the spin exchange scattering rate Γ_s. For small η_0 and $\Gamma_s \ll \Gamma$ the qualitative form of T_c-suppression at small and moderate concentrations will be very similar to the one shown above. For large concentrations, such that $T_c/T_{c0} \ll 1$, the T_c-suppression by the magnetic component in the scattering will be the dominant effect, if $\Gamma_s > 0$. However, one may not treat the

impurities as independent from one another when the impurity concentration is large.

4.5 London Penetration Depth

The opening of the energy gap with increasing impurity concentration is an indelible signature of s-wave superconductivity. It will obviously give rise to activated behavior for $T \ll \Omega_G$ in a wide range of thermodynamic properties, of which we have chosen to discuss only one for purposes of illustration, the temperature-dependent magnetic penetration depth. For the model states and Fermi surface under consideration, this may be expressed as

$$\left(\frac{\lambda_0}{\lambda(T)}\right)^2 = \int d\omega \, \tanh\frac{\beta\omega}{2} \int \frac{d\phi}{2\pi} \, \text{Re} \left\{ \frac{\tilde{\Delta}_k^2}{(\tilde{\omega}^2 - \tilde{\Delta}_k^2)^{3/2}} \right\}, \qquad (4.5)$$

where λ_0 is the pure London result at $T = 0$.

The penetration depth in a d-wave superconductor (Figure 4.8 b) is known to vary as $\lambda(T) \simeq \tilde{\lambda}_0 + c_2 T^2$ at the lowest temperatures [68, 96, 97,73], over a temperature range which widens with increasing impurity concentration. The coefficient c_2 decreases, as Γ^{-1} in the Born limit and $\Gamma^{-1/2}$ in the resonant scattering case. In the anisotropic s-wave case with $\eta_0 > 0$ there is a gradual change in the temperature dependence of the penetration depth at low temperatures. The deviation from the linear behavior of $\lambda(T)$ grows weakly with increasing impurity concentration, see Figure 4.9 . As mentioned earlier the energy gap opens up at $\Gamma_c/T_{c0} \simeq \eta_0(1 + c^2)$.

For $\eta_0 \ll 1$ the corresponding activated behavior in the anisotropic s-wave case is easy to distinguish from the d-wave case when plotted against $(T/T_c)^2$ as also shown in Figure 4.8 . The important experimentally relevant signature is

Figure 4.8 Temperature dependence of normalized magnetic penetration depth $(\lambda_0/\lambda(T))^2$ for s- and d-wave order parameters $(\eta_0 = 0)$vs. reduced temperature $(T/T_c)^2$, shown for various potential scattering rates Γ/T_{c0} in the unitarity limit, $c = 0$.

of course not simply the exponential behavior, but the increase in the activation gap with impurity concentration.

4.6 Effect of Spin Scattering

A simple defect like a vacancy or Zn ion in the CuO_2 plane may not behave simply as a potential scatterer, as assumed above. In the presence of large local
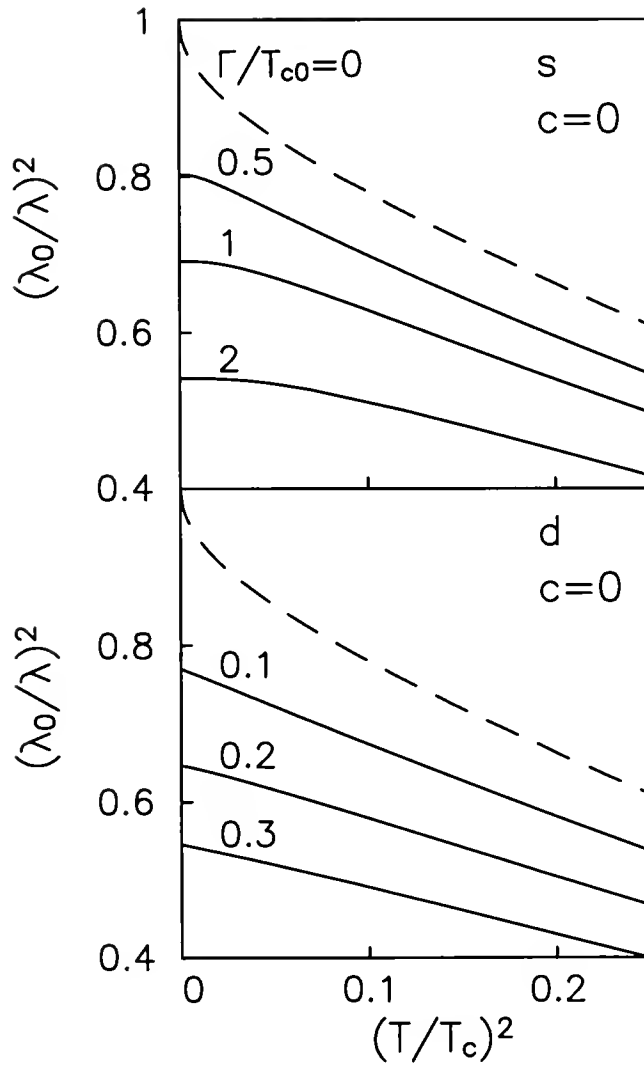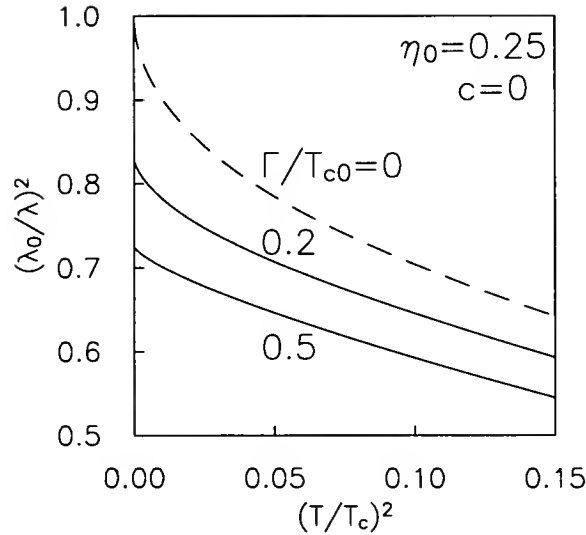
Figure 4.9 Temperature dependence of normalized magnetic penetration depth $(\lambda_0/\lambda(T))^2$ for an order parameter of an extended-s type, with $\eta_0 = 0.25$, in the unitarity limit, $c = 0$.

Coulomb interactions, a magnetic moment may form around the defect site, giving rise to spin-flip scattering of conduction electrons [98]. This poses the most serious obstacle for the direct application of the principle distinguishing d-wave from anisotropic s-wave systems outlined above, since magnetic scattering will lead to gapless superconductivity as in the usual Abrikosov-Gor'kov theory. Furthermore, even if a gap remains, strong spin-flip scattering may lead to bound states within it [66, 99, 100,46] which may give rise under the proper circumstances to a residual density of states $N(\omega \to 0)$ as in the d-wave case. Here we investigate the competition between the opening of the energy gap in the s-wave state due to potential scattering and gapless behavior due to magnetic scattering. To this end we add a term $J\mathbf{S} \cdot \sigma$ to the Hamiltonian, where $\mathbf{S}$ is a classical spin representing the impurity and σ is the conduction electron spin density, and study the system in an average t-matrix approximation analogous to the one applied to the pure potential scattering case. The
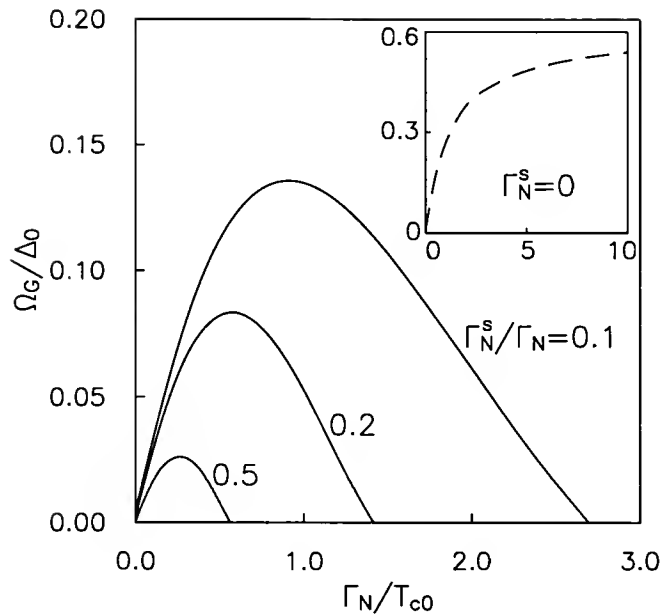
Figure 4.10 Induced energy gap normalized to clean gap maximum, Ω_G/Δ_0, vs. potential scattering rate Γ_N/T_{c0} for different ratios, Γ_N^s/Γ_N, of magnetic to potential scattering rates, $\eta_0 = 0$.

self-energies found in the presence of both types of scattering reduce in the isotropic s-wave case to those given by several authors [46,99, 101]. We find that until the dimensionless exchange JN_0 becomes of $\mathcal{O}(1)$, the results for the s-wave system are very similar to those obtained in the simpler Born approximation, as discussed above, provided η_0 is not large. The self-energies in the Born approximation are $\Sigma_0 = (\Gamma_N + \Gamma_N^s)G_0$ and $\Sigma_1 = (-\Gamma_N + \Gamma_N^s)G_1$ [1], where $\Gamma_N^s \equiv n_i J^2 S(S+1)\pi N_0$. For $\eta_0 = 0$, the induced gap, Ω_G, in the s-wave system may then be shown to vary as $\Omega_G \simeq \Gamma_N - \Gamma_N^s \geq 0$, but the effects of self-consistency rapidly become important as the concentration is increased.

In Figure 4.10 , we plot Ω_G as a function of the impurity concentration through the parameter Γ_N for various assumptions about the scattering character of the impurity ion, where the quantity Γ_N^s/Γ_N specifies the relative amount of magnetic scattering. The destruction of the induced gap takes place because

the system becomes insensitive to large amounts of potential scattering, but magnetic impurities continue to break pairs even at large concentrations. The gap is nevertheless found to persist into the very dirty limit even for systems where the magnetic scattering is nearly as strong as the potential scattering.

For weak spin scattering, the bound state in the t-matrix approximation is found to lie at $\omega \gg \Omega_G$, just below the *average* order parameter Δ_{avg} deep in the continuum, and thus plays no role. Stronger spin scattering does not change this qualitative behavior at low concentrations until $JN_0 \simeq 1$ when the bound state lies at the Fermi level in the classical spin approximation [46]. In this case the Kondo effect, neglected here, also becomes important. It is known from other analyses [102] that the bound state lies near the Fermi level, and will therefore give rise to a residual density of states $N(\omega \to 0)$, only when $T_K \simeq T_c$. For any other ratio of T_K/T_c, the bound state will lie at an energy corresponding to an appreciable fraction of the *average* gap in the system, and hence be irrelevant for our purposes.

Clearly a quantitative estimate of the relative size of Γ and Γ_N^s is required to decide whether spin scattering plays a role in real high-T_c materials with simple defects. Walstedt and co-workers estimated $JN_0 \simeq 0.015$ for a Zn ion in YBCO, implying that Zn is a nearly pure potential scatterer in this system [18]. On the other hand, Mahajan et al. [19] estimate $JN_0 \simeq 0.45$. For a 1% Zn concentration, a magnetic moment of 0.36 μ_B for Zn in fully oxygenated YBCO [19] and a density of states of $1.5/eV$ [19], we find $\Gamma_N^s \simeq 1 \times 10^{-4}$ eV. From the residual resistivities of Zn-doped YBCO crystals [92], we estimate that a 1% Zn sample corresponds to a *total impurity* scattering rate of $\Gamma_N^{imp} \simeq 1 \times 10^{-2} eV$, assuming that the inelastic and elastic contributions to the scattering rate

add incoherently. This suggests that potential scattering must dominate the total elastic rate, $\Gamma_N^s \ll \Gamma$. On the other hand, the large value of $JN_0 \simeq 0.45$ deduced for a Zn ion [19] would mean that the Kondo effect may be important, and that we cannot completely rule out the possibility that a bound state sits very close to the Fermi level. Other experimental results do not support such high values for the magnetic exchange interaction of Zn in YBCO. NMR studies of the Osaka group [80,82] led to the conclusion that $\Gamma_s \ll \Gamma$, and confirm our estimates of Γ_s.

4.7 Microwave Conductivity

Electrical and thermal conductivities, as well as sound attenuation, will be considerably different in extended s– and d-wave states, as suggested by the following argument. Any DC transport coefficient $L(T)$ in a system characterized by well-defined single-particle excitations will vary with temperature roughly as $L(T) \sim N(\omega \simeq T)\tau(\omega \simeq T)$, where $N(\omega)$ is the density of states and $\tau(\omega)$ the relaxation time. In the clean d-wave case, resonant scattering gives $\tau^{-1}(\omega) = 2\Sigma_0''(\omega) \sim N(\omega)^{-1}$ up to logarithmic corrections, yielding $L(T) \sim T^2$. In the Born limit, $c \gg 1$, similar arguments yield $L \sim const.$ for d-wave transport coefficients.

Impurity-limited transport in the extended s-wave state will be qualitatively similar to the d-wave case if the scattering is weak, $c \gg 1$. In contrast to the d-wave case, however, for $c \to 0$ (and $\eta_0 \ll 1$) resonant scattering does not occur, since the denominator of the t-matrix, $c^2 - G_0^2 + G_1^2 \gtrsim (1 - \eta_0)^2$ [79]. A simple low-T estimate accounting for nodal quasiparticle contributions gives $L \sim L_0(1 - 2\eta_0)$ as $T \to 0$. The exact behavior in this range will be
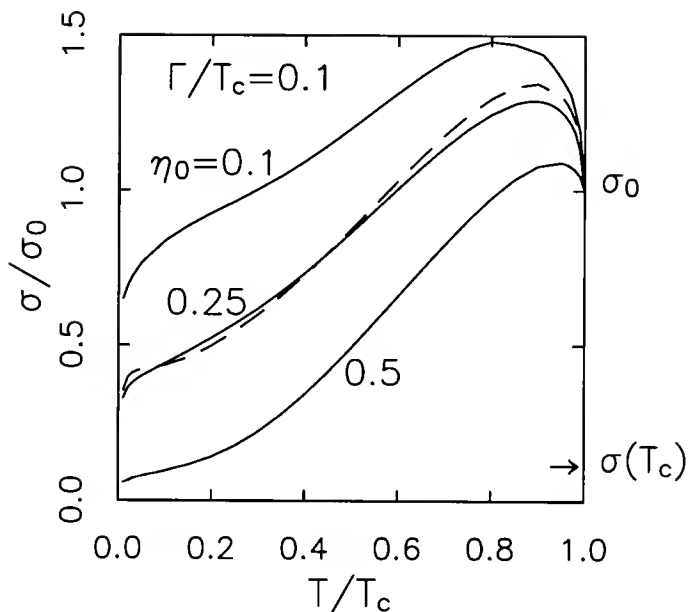
Figure 4.11 Conductivity of extended-s state, Δ_0/T_c=2.92, Γ/T_c=0.1, $c = 0$, η_0=0.1,0.25, and 0.5 (solid lines). Also shown, $\Gamma/T_c = 0.01$, $\eta_0 = 0.25$ (dashed line).

influenced by self-consistency effects and the leading frequency dependence of the t-matrix. The resultant temperature dependence will then be intermediate between the strong and weak scattering limits of d-wave transport coefficients.

In Refs. [103, 104], expressions for the complex conductivity of an anisotropic s-wave superconductor were derived. We do not reproduce these rather lengthy expressions here, but merely comment that a fully self-consistent numerical evaluation confirms the qualitative picture of low-frequency transport described above.

Some typical results are shown in Figure 4.11 for a model in which inelastic scattering has been neglected entirely. The limiting conductivity as $T \rightarrow T_c$ is therefore the impurity Drude result, $\sigma_0 = ne^2/(2m\Gamma_N)$, which for $\Gamma_N \ll T_c$ is much larger than the actual conductivity in the cuprates at the transition, $\sigma(T_c)$, indicated roughly in the figure. At low temperatures $T \ll T_c$,

inelastic scattering may be neglected and the results displayed are valid. The most important qualitative feature of the results is that for $\eta_0 < 2/\pi$, the effective limiting value of the conductivity in the extended-s state is nonzero and generically much larger than $\sigma(T_c)$ in clean high-T_c systems, such that $\bar{\sigma} \equiv \sigma(T \to 0)/\sigma(T_c) \gg 1$. This residual conductivity diminishes as $\eta_0 \to 2/\pi$, when the result should be qualitatively similar to the d-wave conductivity with resonant scattering due to the vanishing of the off-diagonal self-energy. Note, however, that for generic values of η_0, e.g. that apparently appropriate for BSCCO, *the residual conductivity scales inversely with the impurity scattering rate* Γ, in contrast to the resonant d-wave case where the residual conductivity is independent of Γ to leading order.

As shown in Figure 4.11 , the temperature dependence of the conductivity for most of the low temperature range may mimic a linear behavior. This is intriguing, given the linear-T conductivity observed in microwave experiments on clean YBCO crystals [81], but the large residual conductivity predicted (unless η_0 is close to $2/\pi$) would seem to be inconsistent with recent studies indicating that $\sigma(T \to 0)$ is very small in twin-free samples. We are not aware of similar experiments on high-quality BSCCO single crystals. One final point of interest is that the *form* of $\sigma(T)$ is only weakly dependent on disorder, as shown in the figure; of course the overall conductivity scale σ_0 depends inversely on impurity concentration.

The results in the Born approximation are qualitatively similar for both s- and d-wave states, as can be seen from comparison of Figure 4.12 and Figure 2 of Ref. [104]. Note, however, that the clean limit regime in the d-wave state is a much more narrow range of scattering rates than in the s-wave states.

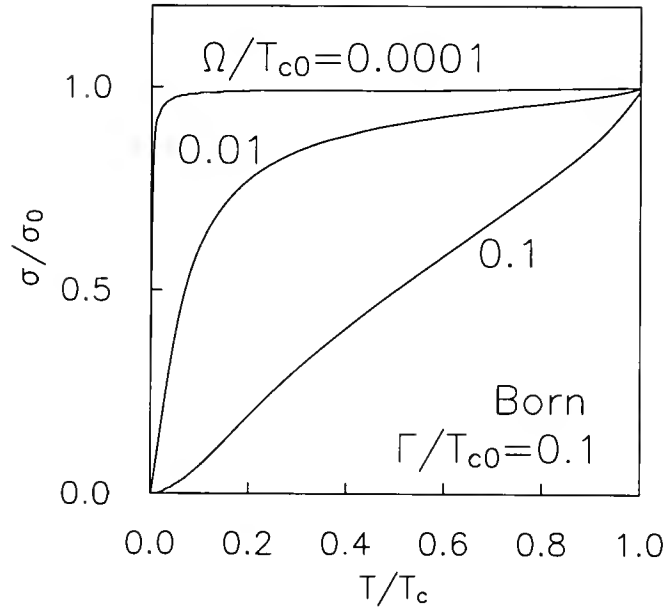**Figure 4.12** Conductivity of extended s-state for several values of external frequency Ω in the Born approximation, $\Delta_0/T_c = 2.92, \Gamma/T_{c0} = 0.1, \eta_0 = 0.25$.
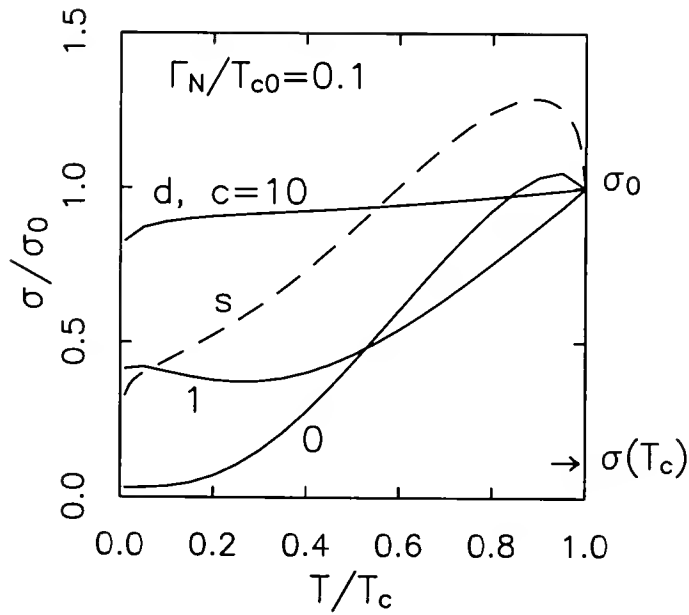

Figure 4.13 Comparison of conductivity of clean extended s-wave state (dashed line), $\eta_0 = 0.25, \Delta_0/T_c = 2.92, \Gamma/T_c = 0.1, c = 0$ with $d_{x^2-y^2}$ state, $\Delta/T_c = 2.14, \Gamma/T_c = 0.1, c = 10, 1$, and 0.

To illustrate the comparison of these results with those expected for a d-wave superconductor, we plot in Figure 4.13 the conductivity in a $d_{x^2-y^2}$ state in the resonant ($c = 0$) and Born ($c = 10$) limits, together with an example of intermediate strength scattering ($c = 1$) chosen to give the same effective $\sigma(T \to 0)$ as the extended-s conductivity for $\eta_0 = 0.25$. Even in the last case the qualitative differences between the s- and d-wave results are manifest. The dependence of the s-wave result on the scattering phase shift and impurity concentration are found to be quite weak, except in the case $c \gg 1$, for which the result is qualitatively similar to the d-wave Born result, since the denominator of the t-matrix becomes irrelevant.

Given the uncertainty regarding the origin of the residual conductivity in the high-T_c materials it is perhaps useful to give estimates for other transport coefficients. For example, since the coherence factors are essentially the same for the electronic thermal conductivity κ_{el}/T as for $\sigma(T)$, it is straightforward to see that the large residual conductivity in the extended s-wave state implies a large linear-T term in the thermal conductivity of order $\frac{1}{6}(1 - 2\eta_0)\gamma v_F^2 T/\Gamma_N$, where v_F is the Fermi velocity and γ is the normal state linear specific heat coefficient. Such a term has not been observed below $2K$ in single crystal BSCCO [105] but there are data at somewhat higher temperatures which are consistent with $\bar{\sigma}_Q \equiv \kappa_{el}(T \to 0)T_c/\kappa_{el}(T_c)T \gg 1$ [106]. The linear term in κ at low T in YBCO appears to be quite small [107].

Very recently the authors of Ref. [108] have pointed out that the "bump" in BSCCO gap function near $\phi = \pi/4$ may be a superlattice effect. In this case available experimental data on BSCCO seem unlikely to be compatible with an anisotropic s-wave state of the type considered here for any η_0.

CHAPTER 5
TWO-CHANNEL KONDO IMPURITIES
IN SUPERCONDUCTORS

In recent years models of fermion systems that cannot be described by a Landau Fermi liquid model received considerable attention. One of those is the two-channel Kondo impurity. In this model conduction electrons described by the flavor α and spin σ interact with impurity spin $S = 1/2$. It was pointed out by and Nozières and Blandin [109] that this model may follow from a realistic description of magnetic impurities in a metal when the orbital structure of the impurity is taken into account. In the two-channel model the impurity spin is overscreened by two exactly degenerate channels of conduction electrons. The new effective spin is $1/2$. This spin couples antiferromagnetically to two other electrons from the two channels, and this process continues as T is lowered. The effective coupling of the conduction band grows in this process and saturates at large, finite values at an intermediate fixed point. The NRG approach shows that the size of the electron cloud around the impurity diverges as $1/T$ when $T \to 0$. The excitation spectrum of this system is not a Fermi liquid. The low temperature magnetic susceptibility and the specific heat coefficient, $\gamma_{imp} \equiv C_{imp}/T$, are logarithmically divergent. Other properties also exhibit non-Fermi liquid behavior below the crossover temperature T_K.

The experimental realization of the two-channel Kondo effect in uranium compounds was proposed but remains controversial [110, 111, 112]. It was argued [110] that in compounds such as UBe_{13} and $Y_{1-x}U_xPd_3$ with $x = 0.2$,

the U ions at crystal sites with cubic symmetry have stable $5f^2$ configuration and $J = 4$ total angular momentum. The crystal-field split $J = 4$ multiplet would have a nonmagnetic Γ_3 doublet as its ground state. In a simplified model this doublet is coupled to an excited doublet in an $5f^1$ configuration, with $J = 5/2$ and Γ_7 symmetry, via hybridization with conduction electron $J = 5/2$, Γ_8 partial waves. A canonical transformation [31,110] yields an effective interaction between the Γ_3 doublet and two channels of conduction states of Γ_8 symmetry.

Here we would like to offer another test of the multichannel Kondo effect. The breaking of time-reversal symmetry involved in scattering by magnetic impurities in superconductors has important consequences. The qualitative type of behavior is well-known in the single channel problem to depend on the ratio T_K/T_{c0}, where T_K is the Kondo temperature and T_{c0} is the transition temperature of a pure superconductor. The divergence of magnetic correlation length and the existence of a residual magnetic moment as $T \to 0$ suggest that in the multichannel case one should expect a very different type of interplay between exchange and pairing interactions.

One may use a sensitivity of superconducting correlations to multichannel exchange interaction as an additional criterion to characterize multichannel Kondo behavior and distinguish it from the single channel case. In this paper we study a simplified SU(N)×SU(k) version of the full multichannel problem in the NCA approximation [113]. Here, N is the orbital degeneracy of the impurity and k is the number of conduction electron channels coupled to the impurity. Although this approach ignores details of anisotropic exchange it remains in the same universality class [113]. In particular the exponents for
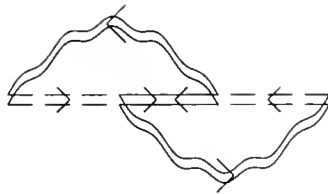
Figure 5.1 The leading order diagram for the anomalous impurity propagator. The dashed lines are the fermion propagators and the wavy and solid lines are boson and conduction electrons respectively.

the temperature dependence of the susceptibilities agree with those obtained from the conformal field theory [110, 114].

Our model includes a BCS pairing of electrons in the conduction band. In general the pairing may be either of channel singlet or triplet type. We assume the latter possibility. The quantities we study in this work are not significantly different for the channel singlet state. In the limit of large on-site Coulomb repulsion U and for temperatures $T \ll U$, the model has a simplified form,

$$
\begin{aligned}
H = &\sum_{k,\alpha,\sigma} \epsilon_k c^\dagger_{k\alpha\sigma} c_{k\alpha\sigma} + E_f \sum_\sigma f^\dagger_\sigma f_\sigma + V \sum_{k,\alpha,\sigma} \left[c^\dagger_{k,\alpha,\sigma} f_\sigma b^\dagger_{\bar\alpha} + h.c. \right] \\
&+ \sum_{k,\alpha,\sigma} \left[\Delta(k) c^\dagger_{k,\alpha,\sigma} c^\dagger_{-k,\alpha,-\sigma} + h.c. \right] + \lambda \left(\sum_\sigma f^\dagger_\sigma f_\sigma + \sum_\alpha b^\dagger_{\bar\alpha} b_{\bar\alpha} - 1 \right).
\end{aligned}
\tag{5.1}
$$

The indices α and σ refer to channel and spin, respectively. The boson $b_{\bar\alpha}$ transforms according to the conjugate representation of SU(k). In the limit $\lambda \to \infty$ the unphysical states with the impurity occupation $n_f > 1$ are projected out. The position of the bare impurity level is assumed to be $E_f = -0.67D$, and $\Gamma = \pi N(0) V^2 = 0.15D$, where D is half of the band width. For this parameter set the Kondo temperature is $T_K = 4.5 \times 10^{-5} D$ and the impurity occupation number is $n_f \simeq 0.9$.

The pairing correlations in the conduction band lead to a nonzero anomalous impurity propagator, $F_{f,\sigma\sigma'}^{\alpha\alpha'}(\tau) = \langle T_\tau f_\sigma(\tau) b_\alpha(\tau) f_{\sigma'}(0) b_{\alpha'}(0) \rangle$ (see Figure 5.1). This propagator, including the internal conduction electron line is evaluated self-consistently at finite impurity concentrations. Although $F_f \sim 1/N^2$, and in NCA only the contributions $O(1/N)$ are retained, F_f is of order $O(\Delta)$ near T_c and must be included in the calculation of the superconducting transition temperature. There are no anomalous contributions to boson and fermion self-energies,

$$\Sigma_0(\omega + i0^+) = NV^2 \int_{-\infty}^{\infty} d\epsilon f(\epsilon) N(\epsilon) G_m(\omega + \epsilon + i0^+), \qquad (5.2)$$

$$\Sigma_m(\omega + i0^+) = kV^2 \int_{-\infty}^{\infty} d\epsilon (1 - f(\epsilon)) N(\epsilon) G_0(\omega - \epsilon + i0^+). \qquad (5.3)$$

Here $k = 2$ is the number of channels. We calculate F_f in the "elastic" approximation [56] in which the internal anomalous conduction electron propagator, see Figure 5.1 , is evaluated at the external frequency. The slope of the initial T_c suppression is obtained by including both diagonal and off-diagonal contributions,

$$\begin{aligned}
-\left(\frac{N_0 dT_c}{dn}\right)_{n=0} &= -\left(\frac{N_0 dT_c}{dn}\right)_1 - \left(\frac{N_0 dT_c}{dn}\right)_2 \\
&= -\frac{N}{2}\pi N_0 V^2 T_{c0}^2 \sum_{n\geq 0}\left[\frac{\text{Im} G_f(\omega_n)}{\omega_n^2} + \frac{F_f(\omega_n)}{\Delta|\omega_n|}\right].
\end{aligned} \qquad (5.4)$$

The detailed form of this formula in the NCA approximation for a single-channel Kondo effect was derived in Ref. [56]. Here we evaluate analogous

expression for the two-channel model. The contribution associated with the impurity spectral function is the following:

$$-\left(\frac{N_0 dT_c}{dn}\right)_1 = \frac{N}{2}\Gamma \int_{-\infty}^{\infty} d\omega \rho_f(\omega) R_1(\omega), \qquad (5.5)$$

where

$$R_1(\omega) = -\frac{T}{\pi\omega^2}\left[\psi(\frac{1}{2}) - \mathrm{Re}\psi\left(\frac{1}{2} + \frac{i\omega}{2\pi T}\right)\right], \qquad (5.6)$$

$$\rho_f(\omega) = \frac{1}{Z_f}(1 + e^{-\beta\omega})\int_{-\infty}^{\infty} d\epsilon e^{-\beta\epsilon}\rho_0(\epsilon)\rho_m(\epsilon + \omega), \qquad (5.7)$$

$$Z_f = \int_{-\infty}^{\infty} d\epsilon e^{-\beta\epsilon}[k\rho_0(\omega) + N\rho_m(\epsilon)], \qquad (5.8)$$

where ψ is the digamma function and ρ_0 and ρ_m are the slave boson and the impurity fermion spectral function, respectively. The second term in equation (5.4) has the following form:

$$-\left(\frac{N_0 dT_c}{dn}\right)_2 = \frac{N}{2}\Gamma \int_{-\infty}^{\infty} d\omega[\sigma_f(\omega) - (m \leftrightarrow)]R_2(\omega), \qquad (5.9)$$

with

$$R_2(\omega) = \frac{T}{4\omega}\left[1 - \frac{2T}{\omega}\tanh\left(\frac{\omega}{2T}\right)\right], \qquad (5.10)$$

$$\sigma_f(\omega) = \frac{1}{Z_f}\int_{-\infty}^{\infty} d\epsilon V(\epsilon; \omega), \qquad (5.11)$$

$$V(\epsilon; \omega) = 4\cosh(\omega/2T)e^{-\beta\epsilon}\mathrm{Re}G_0(\epsilon)\rho_0(\epsilon)$$

$$\times[e^{\beta\omega/2}\rho_m(\epsilon - \omega)\mathrm{Re}G_m(\epsilon + \omega) - e^{-\beta\omega/2}\rho_m(\epsilon + \omega)\mathrm{Re}G_m(\epsilon - \omega)]$$

$$+2\sinh(\omega/T)e^{-\beta\epsilon}[(\mathrm{Re}G_0(\epsilon))^2 - \pi^2\rho_0^2(\epsilon)]\rho_m(\epsilon + \omega)\rho_m(\epsilon - \omega). \qquad (5.12)$$

The expression $(m \leftrightarrow 0)$ indicates the interchange of the fermion and boson indices, m and 0, respectively, in the formula for $\sigma_f(\omega)$. The off-diagonal contribution can be separated into a spin-flip and a spin-preserving part, T_2^{SF} and
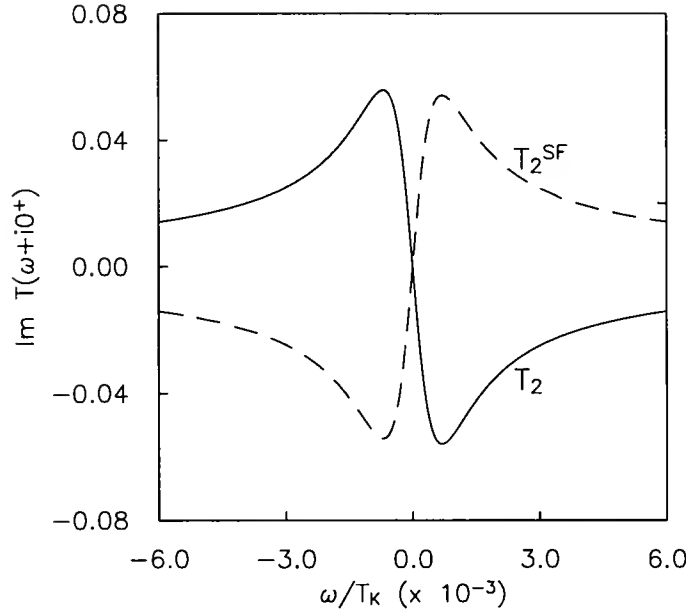
Figure 5.2 The anomalous part of the conduction electron T-matrix evaluated at $T = 4.5 \times 10^{-4} T_K$. The solid (broken) line is the non-spin-flip (spin-flip) contribution.

T_2, respectively. The inclusion of inelastic processes is not expected to significantly affect the results because the spin-flip and non-spin-flip contributions almost cancel [115, 116].

At low temperatures these off-diagonal components of the T-matrix have a peak at $\omega \simeq T$ (see Figure 5.2).

To evaluate T_c-suppression we use the gap equation,

$$1 = V_S \int_0^{\omega_D} d\omega N_0(\omega) \frac{\tilde{\Delta}}{\Delta \tilde{\omega}} \tanh(\omega/2T_c), \qquad (5.13)$$

where $N_0(\omega)$ is the density of conduction electron states in the normal metal and V_S is the pairing potential. The full conduction electron Green's function, averaged over impurity positions, $G^{-1}(\omega) = \tilde{\omega}\tau_0 - \epsilon_k\tau_3 - \tilde{\Delta}(k)\tau_1$, is found from
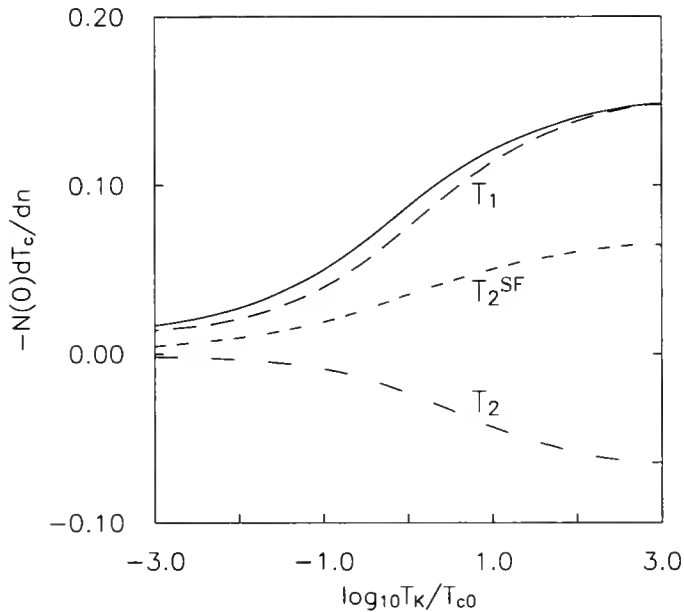
Figure 5.3 The slope of the initial T_c-suppression for a superconductor with two-channel Kondo impurities. The separate contributions come from the diagonal part of the T-matrix, T_1, the off-diagonal spin-flip, T_2^{SF}, and the off-diagonal non-spin-flip, T_2. The solid line is the sum of the three contributions.

the Dyson equations, $\tilde{\omega} = \omega - nV^2 G_f(\tilde{\omega})$, and $\tilde{\Delta} = \Delta + nV^2 F_f(\tilde{\omega})$, where n is impurity concentration.

As shown in Figure 5.3 , the slope $N_0(0)\mathrm{d}T_c/\mathrm{d}n$, at $n = 0$, remains finite as $T_K/T_c \to \infty$, indicating finite pairbreaking in the strong coupling regime. We include for comparison the NCA result for the initial T_c-suppression for a superconductor with single channel Kondo impurities, see Figure 5.4 . The qualitative form of the T_c dependence on n in the two-channel case remains practically unchanged for all values of T_K/T_{c0}, however, as illustrated in Figure 5.5 .

Both results are a consequence of finite magnetic moment of the impurity at all temperatures. The maximum slope is reached for $T_K/T_{c0} \to \infty$, in contrast with the single channel Kondo problem where maximum occurs for $T_K \simeq T_{c0}$.
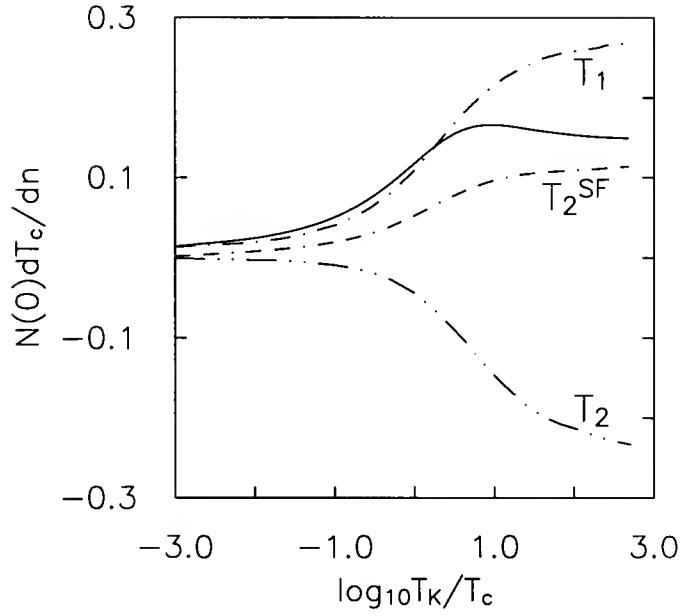
Figure 5.4 The slope of the initial T_c-suppression for a superconductor with single channel Kondo impurities. The separate contributions come from the diagonal part of the T-matrix, T_1, the off-diagonal spin-flip, T_2^{SF}, and the off-diagonal non-spin-flip, T_2. The solid line is the sum of the three contributions.
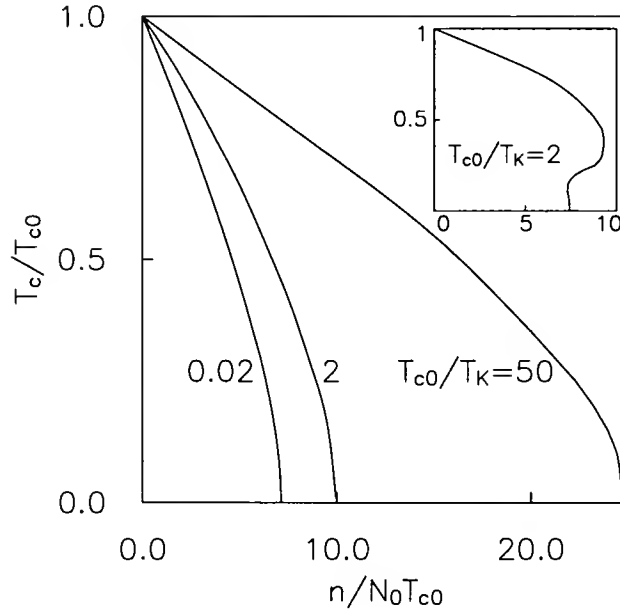

Figure 5.5 The superconducting transition temperature as a function of impurity concentration. The inset shows the result for a single channel Kondo impurity with $T_K \simeq T_c$ evaluated with $E_f = -0.67D$, and $\Gamma = 0.15D$.

Similar results for $(dT_c/dn)_{n=0}$ were obtained in a recent Monte Carlo calculation [115,116]. If the Kondo scale is known from other experiments, measurements of T_c as a function of impurity concentration may help in identifying the multichannel behavior. For $T_{c0} \lesssim T_K$, studies of the single channel problem have found a reentrant or exponential dependence of T_c on concentration. If it were possible to vary the ratio T_K/T_{c0} in the strong coupling regime, increased pairbreaking with growing T_K/T_{c0} would imply multichannel behavior while the opposite would be true for a single channel coupling. In unconventional superconductors, for which $\sum_k F(k,\omega) = 0$, both single and multichannel exchange result in qualitatively similar form of the T_c-dependence on n in the strong coupling regime and the differences which may exist for $T_K \simeq T_{c0}$ may be harder to indentify. Finally, let us note that the breaking of the spin or channel symmetry which takes the system away from the multichannel fixed point should reduce pairbreaking especially in the strong coupling limit. Given the subtleties of this analysis we conclude that T_c-suppression is not likely to be a sensitive tool for identifying the multichannel exchange.

CHAPTER 6
SUMMARY AND CONCLUSIONS

We have studied metals, mainly superconductors, in the presence of magnetic and nonmagnetic impurities. In systems with power law density of states near the Fermi level and antiferromagnetic exchange interaction between impurity and conduction electrons the single impurity calculation in the large-N mean field approximation [3] yields the normalized critical coupling $N_0 J_c \sim r$, at low r, and $N_0 J_c \rightarrow 2$, for $r \rightarrow \infty$. The NCA approach also gives $N_0 J_c \sim r$, for $r \ll 1$. Recent NRG calculations [33] confirm the result for small r but disagree at larger r. There is an upper critical $r_c = 0.5$ for the orbitally non-degenerate single channel Kondo problem, above which the Kondo effect does not occur at all, regardless of the strength of the coupling. The conclusions reached for the same model with nonzero impurity concentration in the mean field approximation are quite different: $J_c = 0$ for any nonzero concentration.

It would be desirable to perform the NCA calculations from chapter 2 in the Coqblin-Schrieffer limit, both at finite temperatures and at $T = 0$. This would allow a closer comparison of this method with the NRG [33] results for the Kondo model with power-law density of states in the conduction band, $N(\omega) \sim |\omega|^r$. In addition to a single-impurity calculation it would be interesting to see the self-consistent NCA treatment for finite concentration of impurities. One would like to know whether in NCA the critical coupling for finite concentrations is $J_c = 0$, as in the mean field approach. Also, it would

be of interest to study the breakdown of the Fermi liquid with increasing r and to use NCA to calculate dynamical quantities.

In chapter 3 we have presented a slave boson theory of Kondo impurities in superconductors which has the advantages of being applicable in the Fermi liquid regime and being relatively easy to use in calculating quantities of experimental interest at all temperatures in the superconducting state. The theory has been shown to reproduce all of the qualitative features of the physics found by previous theories for large T_K, and is asymptotically in quantitative agreement with "exact" NRG calculations for the s-wave case. It is furthermore capable of going considerably beyond currently available theories in that practical calculations of superconducting response functions are possible at low temperatures in the superconducting state, and can be easily generalized to the unconventional states of great current interest in the heavy fermion and high-temperature superconductivity problems.

The single exception to this success is the failure to properly describe the s-wave superconductor at very large impurity concentrations, in that the theory predicts an infinite critical concentration. In practical terms this is quite academic, as all independent impurity analyses will break down due to inter-impurity interaction effects long before any putative critical concentration is achieved. Nevertheless, this formal shortcoming of the theory exists and must be addressed. Preliminary analysis of fluctuations about the saddle point has convinced us that the Gaussian fluctuations to the scattering amplitude arising from the slave boson dynamics will be sufficient to induce a critical concentration, in analogy to the works of Matsuura et al. [52] and Sakurai [53], and that

the theory as it stands is sufficient to describe the Fermi liquid regime everywhere except for very large concentrations in the s-wave case. The difficulty does not arise in the unconventional case.

In unconventional superconductors, we have shown that the phenomenological theories of Refs. [5] and [6] will be reproduced by the microscopic theory presented here in the limit $N = 2$ and $T_K/T_c \to \infty$. The decondensation of the slave boson amplitude prevents extension of the theory into the high temperature regime, but qualitatively it is clear that the effect of lowering the Kondo temperature is to sharpen the many-body resonance near the Fermi surface, but lower its weight. Thus the effect of resonant scattering leading to low-energy gapless effects in superconducting thermodynamic and transport properties is reduced. Impurities with larger orbital degeneracy may lead to similar resonances away from the Fermi level, possibly similar to those observed by Maple et al. [117] in specific heat experiments on Pr-doped YBCO.

The effect of Zn and Ni-doping on superconducting properties of YBCO suggests that these two dopants may be described within a traditional Kondo-type picture in conjunction with the theory discussed here. Ni, with spin one, may possibly be treated as a higher-degeneracy scatterer below its Kondo temperature. As we have seen, such an impurity acts as a weak scatterer compared to the $N = 2$, $T_K \gg T_c$ resonant scattering case, a possible model for Zn. On the other hand, recent NMR measurements appear to suggest that a moment forms around the Zn site. Within an isolated impurity picture, this would suggest that $T_K \ll T_c$, where the present theory is not applicable. A more plausible explanation, however, is that the local spin correlations induced

by a missing Cu must be accounted for, as suggested by Poilblanc et al. [98] Further experimental and theoretical work on this problem is clearly essential.

There is by now a considerable body of experimental data supporting the picture of gapless superconductivity in the cuprate high-T_c materials, with a residual density of states and low-temperature behavior varying qualitatively according to the d-wave plus resonant scattering model [16, 118,80,17]. This data stands in apparent contradiction to the well-known effect of small amounts of potential scatterers on anisotropic s-wave superconductors, namely the smearing of energy gap anisotropy. This continues to hold even for extremely anisotropic systems with nodes, as illustrated by the simple theory presented here for a representative order parameter. We believe that this data strongly suggests that the pairing is unconventional in these materials, but the analysis presented in chapter 4 does not as it stands allow one to distinguish among possible candidate unconventional states (e.g., $d_{x^2-y^2}$ and d_{xz}) without further quantitative comparison. It should be noted that time-reversal breaking unconventional states with a gap will become gapless in the presence of pure potential scattering.

As we have briefly discussed in chapter 4, the major difficulty inherent in such an analysis is the possibility that even an apparently "inert" impurity such as Zn or a vacancy in the Cu-O planes may induce local spin correlations in the strongly interacting electron system, leading to spin-flip scattering. Ruling out gapless superconductivity induced by magnetic scattering then becomes a quantitative problem. Gapless behavior in films suggests that a resonant scattering mechanism of some type must be present in order to induce a significant residual density of states with comparatively little T_c suppression. We have

shown, however, that resonant potential scattering does not take place in s-wave systems, and argued that low-energy resonant spin scattering is much less likely than in the isotropic case. We have furthermore made a crude estimate of the importance of spin-flip scattering in Zn-doped YBCO crystals which indicates these materials are dominated by potential scattering and should therefore exhibit an induced gap if the superconducting state is s-wave.

We have also shown that, although gapless behavior in thermodynamic quantities qualitatively similar to d-wave states is to be expected for a range of impurity concentrations in extended-s states, transport properties are quite different in the two states. In particular, residual $T \to 0$ conductivities (σ and κ/T) are expected to be large and to scale inversely with impurity concentration, in contrast to the resonant d-wave case. Such experiments can therefore be used in conjunction with Josephson measurements to settle the question of order parameter symmetry. Existing transport data on YBCO single crystals appear to restrict possible s-states to those where the average of the order parameter over the Fermi surface is nearly zero. The ARPES experiments on the BSCCO–2212 material might imply a strongly anistropic s-wave order parameter with $\eta_0 \simeq 0$. The existing transport measurements, however, do not support this interpretation. Further measurements on the latter system, particularly systematic doping studies to search for an impurity-induced gap and to test impurity scaling of residual conductivities can help to distinguish s- and d-wave state. A careful determination of the temperature dependence of κ over the $1K - 30K$ range in BSCCO would be of great value in this regard.

In chapter 5 we studied the effect of two-channel Kondo impurities on superconducting states. This type of impurity is known to have a non-Fermi

liquid ground state in a normal metal. Since the impurity never loses its magnetic moment due to overscreening by conduction electrons, even in the strong coupling regime, it is not surprising that we find qualitatively similar type of T_c dependence on impurity concentration for all values of T_K/T_c. The initial slope of T_c suppression does vary greatly, however, reaching its maximum as $T_K/T_c \to \infty$. There is no reentrant behavior of T_c as a function of n. One should remember, however, that the impurity screening radius diverges as $T \to 0$ in the two-channel problem. Therefore, below a certain temperature impurities cannot be treated as being independent from one another. In principle the character of the superconducting response in the regime $T \lesssim T_K$ might help to distinguish a two-channel Kondo impurity from a single channel one, provided we know the symmetry of the order parameter of the superconducting host.

REFERENCES

[1] A.A. Abrikosov and L.P. Gor'kov, Zh. Eksp. Teor. Fiz. **39**, 1781 (1960) [Sov. Phys. JETP **12**, 1243 (1961)].

[2] P.W. Anderson, J. Phys. Chem. Solids **11**, 26 (1959).

[3] D. Withoff and E. Fradkin, Phys. Rev. Lett. **64**, 1835 (1990).

[4] K. Ueda and T.M. Rice, in *Theory of Heavy Fermions and Valence Fluctuations*, edited by T. Kasuya and T. Saso (Springer, Berlin, 1985).

[5] P.J. Hirschfeld, D. Vollhardt, and P. Wölfle, Solid State Commun. **59**, 111 (1986).

[6] S. Schmitt-Rink, K. Miyake, and C.V. Varma, Phys. Rev. Lett. **57**, 2575 (1986).

[7] P. Nozières, J. Low Temp. Phys. **17**, 31 (1974).

[8] E. Müller-Hartmann and H. Shiba, Z. Phys. **23**, 143 (1976).

[9] W.N. Hardy, D.A. Bonn, D.C. Morgan, R. Liang, and K. Zhang, Phys. Rev. Lett. **70**, 3999, (1993).

[10] Z.-X. Shen, D.S. Desson, B.O. Wells, D.M. King, W.E. Spicer, A.J. Arko, D. Marshall, L.W. Lombardo, A. Kapitulnik, P. Dickinson, S. Doniach, J. DiCarlo, A.G. Loeser, and C.H. Park, Phys. Rev. Lett. **70**, 1553 (1993).

[11] R.J. Kelley, J. Ma, G. Margaritondo, and M. Onellion, Phys. Rev. Lett. **71**, 4051 (1993).

[12] D.A. Wollman, D.J. van Harlingen, W.C. Lee, D.M. Ginsberg, and A.J. Leggett, Phys. Rev. Lett. **71**, 2134 (1993).

[13] D.A. Brawner and H.R. Ott, Phys. Rev. B **50**, 6530 (1994).

[14] C.C. Tsuei, J.R. Kirtley, C.C. Chi, L.S. Yu-Jahnes, A. Gupta, T. Shaw, J.Z. Sun, and M.B. Ketchen, Phys. Rev. Lett. **73**, 593 (1994).

[15] A. Mathai, Y. Gim, R.G. Black, A. Amar, and F.C. Wellstood, Phys. Rev. Lett. **74**, 4523 (1995).

[16] K. Ishida, Y. Kitaoka, T. Yoshitomi, N. Ogata, T. Kamino, and K. Asayama, Physica C **179**, 29 (1991).

84

[17] D. Achkir, M. Poirier, D.A. Bonn, R. Liang, and W.N. Hardy, Phys. Rev. B **48**, 13 184 (1993).

[18] R.E. Walstedt, R.F. Bell, L.F. Schneemeyer, J.V. Waszczak, W.W. Warren, R. Dupree, and A. Gencten, Phys. Rev. B **48**, 10646 (1993).

[19] A.V. Mahajan, H. Alloul, G. Collin, and J.F. Marucco, Phys. Rev. Lett. **72**, 3100 (1994).

[20] S.E. Barnes, J. Phys. F **6**, 1375 (1976).

[21] P. Coleman, Phys. Rev. B **28**, 5255 (1983).

[22] N. Read and D.M. Newns, J. Phys. C **16**, 3273 (1983).

[23] L.S. Borkowski and P.J. Hirschfeld, Phys. Rev B **46**, 9274 (1992).

[24] L.S. Borkowski and P.J. Hirschfeld, J. Low Temp. Phys. **96**, 185 (1994).

[25] L.S. Borkowski and P.J. Hirschfeld, Phys. Rev. B **49**, 15404 (1994).

[26] L.S. Borkowski and P.J. Hirschfeld, Physica B **206-207**, 183 (1995).

[27] L.S. Borkowski, P.J. Hirschfeld, and W.O. Putikka, Phys. Rev. B, to appear (1995).

[28] K.G. Wilson, Rev. Mod. Phys. **47**, 773 (1975).

[29] H. R. Krishnamurthy, J.W. Wilkins, and K.G. Wilson, Phys. Rev. B **21**, 1003 (1980).

[30] P.W. Anderson, J. Phys. C **3**, 2436 (1970).

[31] J.R. Schrieffer and P.A. Wolff, Phys. Rev. **149**, 491 (1966).

[32] B. Coqblin and J.R. Schrieffer, Phys. Rev. **185**, 847 (1969).

[33] K. Ingersent, unpublished, (1995).

[34] T. Saso, J. Phys. Soc. Japan **61**, 3439 (1992).

[35] T. Saso and J. Ogura, Physica B **186-188**, 372 (1993).

[36] J. Ogura and T. Saso, J. Phys. Soc. Japan **62**, 4364 (1993).

[37] K. Takegahara, Y. Shimizu, and O. Sakai, J. Phys. Soc. Japan **61**, 3443 (1992).

[38] K. Takegahara, Y. Shimizu, N. Goto, and O. Sakai, Physica B **186-188**, 381 (1993).

[39] H. Keiter and G. Morandi, Phys. Rep. **109**, 227 (1984).

[40] N.E. Bickers, Rev. Mod. Phys. **59**, 845 (1987).

[41] E. Müller-Hartmann, Z. Phys. B **57**, 281 (1984).

[42] S. Inagaki, Prog. Theor. Phys. **62**, 1441 (1979).

[43] Y. Kuramoto and H. Kojima, Z. Phys. B **57**, 95 (1984).

[44] A.M. Tsvelick and P.B. Wiegmann, Adv. Phys. **32**, 453 (1983).

[45] E. Müller-Hartmann, in *Magnetism*, vol V., ed. H. Suhl (Academic Press: New York, 1973), and references therein.

[46] H. Shiba, Prog. Theor. Phys. **40**, 435 (1968)

[47] E. Müller-Hartmann and J. Zittartz, Z. Physik **234**, 58 (1970).

[48] Y. Nagaoka, Phys. Rev. **138A**, 1112 (1965).

[49] G. Riblet and K. Winzer, Solid State Commun. **9**, 1663 (1971).

[50] M.B. Maple, W.A. Fertig, A.C. Mota, L.E. DeLong, D. Wohlleben, and R. Fitzgerald, Solid State Commun. **11**, 829 (1972).

[51] P.H. Ansari, J.B. Bulman, J.G. Huber, L.E. DeLong, and M.B. Maple, Phys. Rev. B **49**, 3894 (1994).

[52] T. Matsuura, S. Ichinose, and Y. Nagaoka, Prog. Theor. Phys. **57**, 713 (1977).

[53] A. Sakurai, Phys. Rev. B **17**, 1195 (1978).

[54] K. Yosida and K. Yamada, Prog. Theor. Phys. **53**, 1286 (1975).

[55] S. Ichinose, Prog. Theor. Phys. **58**, 404 (1977).

[56] N.E. Bickers and G. Zwicknagl, Phys. Rev. B **36**, 6746 (1987).

[57] M. Jarrell, Phys. Rev. Lett. **61**, 2612 (1988).

[58] O. Sakai, Y. Shimizu, H. Shiba, and K. Satori, J. Phys. Soc. Japan **62**, 3181 (1993).

[59] P. Schlottmann, J. Low Temp. Phys. **47**, 27 (1982).

[60] M.B. Maple, L.E. Long and B.C. Sales, in *Handbook on the Physics and Chemistry of Rare Earths*, ed. K.A. Gschneider, Jr. and L. Eyring (North-Holland, 1978).

[61] T. Matsuura, Prog. Theor. Phys. **57**, 1823 (1977).

[62] J. Zittartz and E. Müller-Hartmann, Z. Physik **232**, 11 (1970).

[63] M. Jarrell, D.S. Sivia and B. Patton, Phys. Rev. B **42**, 4804 (1990).

[64] A. Sakurai, Physica B **86-88**, 521 (1977).

[65] S. Skalski, O. Betbeder-Matibet, and P.R. Weiss, Phys. Rev. **136** A 1500 (1964).

[66] T. Soda, T. Matsuura, and Y. Nagaoka, Prog. Theor. Phys. **38**, 551 (1967).

[67] C.M. Varma, Comments in Solid State Physics **11**, 221 (1985).

[68] F. Gross, B.S. Chandrasekhar, D. Einzel, K. Andres, P.J. Hirschfeld, H.R. Ott, J. Beuers, Z. Fisk, and J.L. Smith, Z. Phys. B **64**, 175 (1986).

[69] L.P. Gor'kov and P.A. Kalugin, Pis'ma Zh. Eksp. Teor. Fiz. **41**, 208 (1985) [JETP Lett. **41**, 253 (1985)].

[70] P.J. Hirschfeld, P. Wölfle, and D. Einzel, Phys. Rev. B **37**, 83 (1988).

[71] E.A. Schuberth, B. Stricker, and K. Andres, Phys. Rev. Lett. **68**, 117 (1992).

[72] C.H. Choi and P. Muzikar, Phys. Rev. B **37**, 5947 (1988).

[73] P.J. Hirschfeld and N. Goldenfeld, Phys. Rev. B **48** (1993).

[74] H. Kim, G. Preosti, and P. Muzikar, Phys. Rev. B **49**, 3544 (1994).

[75] H. Ding, J.C. Campuzano, A. F. Bellman, T. Yokoya, M.R. Norman, M. Randeria, T. Takahashi, H. Katayama-Yoshida, T. Mochiku, K. Kadowaki, and G. Jennings, Phys. Rev. Lett. **74**, 2784 (1995).

[76] M.R. Norman, M. Randeria, H. Ding, and J.C. Campuzano, preprint (1995).

[77] P.A. Lee and K. Kuboki, preprint (1995).

[78] R. Fehrenbacher and M.R. Norman, Physica C **235-240**, 2407 (1994).

[79] R. Fehrenbacher and M. Norman, Phys. Rev. B **50**, 3495 (1994).

[80] See K. Ishida, Y. Kitaoka, N. Ogata, T. Kamino, K. Asayama, J.R. Cooper, and N. Athanassapoulou, J. Phys. Soc. Jpn. **62**, 2803 (1993), and references therein.

[81] See D.A. Bonn, S. Kamal, K. Zhang, R. Liang, D.J. Baar, E. Klein, and W.N. Hardy, Phys. Rev. B **50**, 4051 (1994), and references therein.

[82] Y. Kitaoka, K. Ishida, G.-q. Zheng, H. Tou, K. Magishi, S. Matsumoto, K. Yamazoe, H. Yamanaka, and K. Asayama, J. Phys. Chem. Solids, in press.

[83] T.P. Deveraux, D. Einzel, B. Stadlober, R. Hackl, D.H. Leach, and J.J. Neumeier, Phys. Rev. Lett. **72**, 396 (1994).

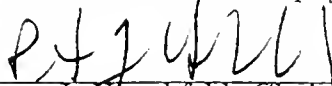[84] P. Arberg, M. Mansor and J.P. Carbotte, Solid State Commun. **86**, 671(1993).

[85] T. Hotta, J. Phys. Soc. Japan, **62**, 274 (1993).

[86] M. Prohammer and J. Carbotte, Phys. Rev. B **43**, 5370 (1991).

[87] P. Monthoux and D. Pines, Phys. Rev. B **49**, 4261 (1994).

[88] V.B. Geshkenbein and A.I. Larkin, Pis'ma Zh. Eksp. Teor. Fiz. **43**, 306 (1986)[JETP Lett. **43**, 395 1986)].

[89] M. Sigrist and T.M. Rice, J. Phys. Soc. Jpn. **61**, 4283 (1992).

[90] Z.-X. Shen, Proceedings of the Conference on Spectroscopies on Novel Superconductors, Stanford 1995.

[91] C.J. Pethick and D. Pines, Phys. Rev. Lett. **50**, 270 (1986).

[92] T.R. Chien, Z.Z. Wang, and N.P. Ong, Phys. Rev. Lett. **67**, 2088 (1991).

[93] T. Tsuneto, Prog. Theor. Phys. **28**, 857 (1962).

[94] D. Markowitz and L.P. Kadanoff, Phys. Rev. **131**, 563 (1963).

[95] P. Hohenberg, Zh. Eksp. Teor. Fiz. **45**, 1208 (1963) [Sov. Phys. JETP **18**, 834 (1964)].

[96] C.H. Choi and P. Muzikar, Phys. Rev. B **39**, 11296 (1989).

[97] R.A. Klemm, K. Scharnberg, D. Walker, and C.T. Rieck, Z. Phys. B **72**, 139 (1988).

[98] D. Poilblanc, D.J. Scalapino, W. Hanke, Phys. Rev. Lett. **72**, 884 (1994).

[99] A.I. Rusinov, Zh. Eksp. Teor. Fiz. **56**, 2047 (1969) [Sov. Phys. JETP **29**, 1101 (1969)].

[100] K. Maki, Phys. Rev. **153**, 428 (1967).

[101] Y. Okabe and A.D.S. Nagi, Phys. Rev. B **28**, 1320 (1983).

[102] J. Kondo, Prog. Theor. Phys. **32**, 37 (1964).

[103] P.J. Hirschfeld, W.O. Putikka, and D.J. Scalapino, Phys. Rev. Lett. **71**, 3705 (1993).

[104] P.J. Hirschfeld, W.O. Putikka, and D.J. Scalapino, Phys. Rev. B **50**, 10250 (1994).

[105] D.-M. Zhu, A.C. Anderson, E.D. Bukowski, and D.M. Ginsberg, Phys. Rev B **40**, 841 (1989).

[106] C. Uher in *Physical Properties of High Temperature Superconductors*, vol. 3, D. Ginsberg, ed. (World Scientific, Singapore, 1992).

[107] L. Taillefer, private communication.

[108] M.R. Norman, M. Randeria, H. Ding, J.C. Campuzano, and A.F. Bellman, Phys. Rev. B **52**, 615 (1995).

[109] P. Nozières and A. Blandin, J. Phys. **41**, 193 (1980).

[110] D.L. Cox, Phys. Rev. Lett. **59**, 1240 (1987).

[111] C.L. Seaman, M.B. Maple, B.W. Lee, S. Ghamaty, M.S. Torikashvili, J.-S. Kang, L.Z. Liu, J.W. Allen, and D.L. Cox, Phys. Rev. Lett. **67**, 2882 (1991).

[112] B. Andraka and A. Tsvelik, Phys. Rev. Lett. **67**, 2886 (1991).

[113] D.L. Cox, A.E. Ruckenstein, Phys. Rev. Lett. **71**, 1613 (1993).

[114] I. Affleck and A.W.W. Ludwig, Nucl. Phys. B**360**, 641 (1991).

[115] K.-H. Luk, Ph.D. Thesis, Ohio State University, 1992.

[116] K.-H. Luk, M. Jarrell, and D.L. Cox, Phys. Rev. B **50**, 15 864 (1994).

[117] S. Ghamaty, B.W. Lee, J.J. Neumeier, and M.B. Maple Phys. Rev. B **43**, 5430 (1991).

[118] J.A. Martindale, K.E. O'Hara, S.M. DeSoto, C.P. Slichter, T.A. Friedmann, and D.M. Ginsberg, Phys. Rev. Lett. **68**, 702 (1992).

BIOGRAPHICAL SKETCH

Lech S. Borkowski was born in 1963 in Kętrzyn, Poland. He attended Szkoła Podstawowa Nr 1 and Liceum Ogólnokształcące in Kętrzyn. He studied chemistry at the Nicolaus Copernicus University in Toruń and Warsaw University of Technology for one year and a half. Later he studied physics at the Wrocław University of Technology and received his M.S. degree there in 1987. He then went to the United States and studied at the Virginia Polytechnic Institute and State University in Blacksburg, Virginia, before transferring to the University of Florida, Gainesville, where he did his research with the Condensed Matter Theory Group at the Physics Department, under the supervision of Prof. Peter Hirschfeld.
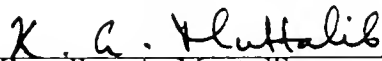
I certify that I have read this study and that in my opinion it conforms to acceptable standards of scholarly presentation and is fully adequate, in scope and quality, as a dissertation for the degree of Doctor of Philosophy.

Peter J. Hirschfeld, Chair
Associate Professor of Physics

I certify that I have read this study and that in my opinion it conforms to acceptable standards of scholarly presentation and is fully adequate, in scope and quality, as a dissertation for the degree of Doctor of Philosophy.
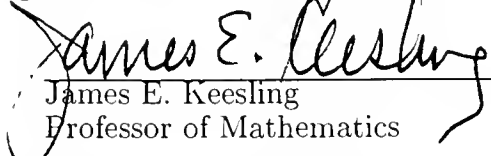
Pradeep Kumar
Professor of Physics

I certify that I have read this study and that in my opinion it conforms to acceptable standards of scholarly presentation and is fully adequate, in scope and quality, as a dissertation for the degree of Doctor of Philosophy.

Kevin Ingersent
Associate Professor of Physics

I certify that I have read this study and that in my opinion it conforms to acceptable standards of scholarly presentation and is fully adequate, in scope and quality, as a dissertation for the degree of Doctor of Philosophy.

Khandker A. Muttalib
Associate Professor of Physics

I certify that I have read this study and that in my opinion it conforms to acceptable standards of scholarly presentation and is fully adequate, in scope and quality, as a dissertation for the degree of Doctor of Philosophy.

James E. Keesling
Professor of Mathematics

This dissertation was submitted to the Graduate Faculty of the Department of Physics in the College of Liberal Arts and Sciences and to the Graduate School and was accepted as partial fulfillment of the requirements for the degree of Doctor of Philosophy.

August 1995

Dean, Graduate school